

Abundances Stratification of Exoplanet Host Stars

C. Saffe¹, H. Levato¹, Z. López-García², E. Jofré², R. Petrucci², and E. González²

¹ Complejo Astronómico El Leoncito, CC 467, 5400 San Juan, Argentina
e-mail: csaffe@casleo.gov.ar, hlevato@casleo.gov.ar, zlgarcia@casleo.gov.ar

² Facultad de Ciencias Exactas, Físicas y Naturales (UNSJ), 5400 San Juan, Argentina
e-mail: emiliano_jofre@yahoo.com.ar, romina_petracci@yahoo.com.ar, chimangolatino@hotmail.com

Received September 15, 1492; accepted October 16, 1492

ABSTRACT

Aims. To determine Σ (variation of Fe abundance with the optical depth), τ_{FeI} , τ_{FeII} (Rosseland median optical depth of Fe lines) and $\Delta[Fe/H](=[FeI/H]-[FeII/H])$, in 79 Exoplanet Host stars (66 main sequence and 13 giants), with respect to 322 solar neighborhood field stars (9 main sequence and 313 giant stars).

Methods. We derived FeI and FeII abundances using equivalent width measurements together with ATLAS9 (Kurucz 1993) model atmospheres and the WIDTH9 program.

Results. The Rosseland median optical depths τ_{FeI} and τ_{FeII} are dependent on stellar parameters ($\log g$, T_{eff} and ξ). We conclude that Σ is a more reliable stratification indicator than τ_{FeI} , τ_{FeII} and $\Delta[Fe/H]$. Our results show that statistically most EH stars (main sequence and giants) have an stratification similar to field stars, which is in agreement with the primordial hypothesis of metal enhancement. The lack of correlation between Σ and the exoplanet parameters (minimum mass, semiaxis and eccentricity) for most of the EH stars, and between $[FeI/H]$ and Σ , favors the primordial hypothesis of metal-enrichment. However, we cannot discard that some EH stars (and even non-EH stars) have suffered and accretion process in the past. We consider candidate stars with stratified atmospheres those with $\Sigma < 0$: 20% (13/65) main sequence EH stars and 33% (4/12) giant EH stars. The group of candidate main sequence stars with stratified atmospheres ($\Sigma < 0$), seems to show a correlation with $[FeI/H]$, which probably relate the stratification in these stars with accretion events. Finally, our sample of 13 giant exoplanet host stars present solar metallicity values (median = -0.09 dex).

Key words. Techniques: spectroscopic – Stars: abundances – Stars: late-type

1. Introduction

The group of main sequence stars with giant planets are, on average, metal-rich in comparison to stars that do not harbor Doppler-detected planets (see, for example, Santos et al. 2004, 2005). On the other hand, Pasquini et al. (2007) compared the metallicities of giant and dwarf stars with giant planets and found that the first group has, on average, lower metallicities than the dwarfs. Hekker & Meléndez (2007) do not confirm Pasquini et al.’s result, although both works studied relatively small samples (14 and 20 objects, respectively). The metallicity trend of giant stars with giant planets remains an open issue for the time being. The planet mass also seems to play a role. Neptune-like or super-Earth planets do not form preferentially around metal-rich stars (e.g. Udry et al. 2006; Sousa et al. 2008).

The excess metallicity of exoplanet host (EH) stars is usually explained by two hypothesis (e.g. González 2006): a primordial origin, and the accretion scenario. In the first case the “excess” of metallicity was already present in the parent cloud from which the star-bearing planet was formed (see, for example, Santos et al. 2001). In the pollution scenario the convective zone (CZ) of the star is contaminated by the infall or accretion of planets and/or planetesimals (see, for example, González et al. 2001).

The CZ of stars acts as a material diluting medium. In main sequence stars, hot F dwarfs should exhibit thinner CZs than cold G dwarfs, i.e. a dependence of CZ with temperature. Also, giant stars have larger CZ than main sequence stars, i.e. a dependence of CZ with luminosity class. If the photosphere of an

star accreted metal-rich material, the upper layers would exhibit a metal excess, while deeper layers should have the lower initial metallicity. Then, the CZ could mix the metal content of upper and lower layers, and consequently different stars should present a different degree of pollution. For example, main sequence EH stars would show more stratified atmospheres than giant EH stars.

The accretion hypothesis of metal excess has been tested using these facts. Santos et al. (2004) found a lack of correlation between the thickness of the convective zone and the metallicity for a sample of FG dwarfs with planets. In this case, the pollution hypothesis is not favored by these observations and the primordial origin of the metal excess remains an alternative. On the other hand, we mentioned the Pasquini et al. (2007) result that giant EH stars shows solar metallicities, without excess like main sequence EH stars. In this case, the pollution scenario is favored (over the primordial origin) since it can explain the observed difference in metallicities between dwarfs and giants with planets. Then, the origin or the cause of the “excess” of metallicity of stars with giant planets is not well understood.

This work is an attempt to statistically study the stratification properties of EH stars and the accretion/primordial hypothesis of metal excess. We study the limitations of four different stratification indicators: Σ (variation of Fe abundance with the optical depth), τ_{FeI} , τ_{FeII} (Rosseland median optical depth of Fe lines) and $\Delta[Fe/H](=[FeI/H]-[FeII/H])$. If the primordial hypothesis is valid, then main sequence and giant EH stars all should present, on average, non-stratified atmospheres. On the other hand, if the accretion hypothesis is valid, different stars would present differ-

ent degree of stratification, due to their different CZs. Also, we want to address the question if EH stars have different stratification properties compared to non-EH solar neighborhood stars, and the possible relation between stratification and exoplanet parameters (minimum mass $M \sin i$, eccentricity e and semiaxis a).

2. Observations and data reduction

We observed 29 southern hemisphere EH stars from the California and Carnegie Planet Search¹ and the Geneva Observatory Planet Search² lists. These compilations basically include 273 EH stars up to September 24, 2008 including 313 exoplanets and 30 multiple systems. 252 EH stars have been detected by Doppler spectroscopy and 52 by photometry. The likely planetary companions have masses such that $M \sin i < 15 M_{JUP}$. The stars we observed have distances between 10 and 94 pc and spectral types F, G, and K (8, 19, and 2 objects, respectively), as specified in the Hipparcos database.

Table 1 present the list of all stars studied in this work, including their fundamental parameters, an identification if they are EH stars or not, and if they are giants or not. In particular, the sample of stars observed in this work are identified in the last column of the Table with "This work". We complemented with literature data (equivalent widths) and increased significantly the number of stars studied in this research. These reference papers are identified with R1,...,R11 in Table 1 (González 1998; González et al. 1999, 2001; González & Laws 2000; Laws & González 2001; Laws et al. 2003; Sadakane et al. 2005; Santos et al. 2000; Zhao et al. 2002; Takeda et al. 2005, 2008).

The stellar spectra of our sample stars were obtained at Complejo Astronómico El Leoncito (CASLEO). We used *Jorge Sahade* 2.15-m telescope equipped with a REOSC echelle spectrograph³ and a TEK 1024×1024 CCD detector. The REOSC spectrograph uses gratings as cross dispersers. We used a grating with 400 lines mm⁻¹, covering the spectral range $\lambda\lambda 3500$ –6500, giving a resolving power of ~ 12500 . Three individual spectra for each object were obtained in four observing runs: August 05–08 2005, August 18–22 2005, February 18–25 2006 and May 04–07 2007 and have S/N ratio of about 300.

The spectra were reduced using IRAF⁴ standard procedures for echelle spectra. We applied bias and flat corrections and then normalized order by order with the *continuum* task, using 7–9 order Chebyshev polynomials. We also corrected by the scattered light in the spectrograph (*apscatter* task). We fitted the background with a linear function on both sides of the echelle apertures, using the task *apall*. The resolution of the reduced spectra is 0.17 Å/pix. Extensive description of the characteristics of the observational material, the reduction technique and some results obtained with it, have been previously published (Saffe et al. 2008, 2005, 2004).

The equivalent widths were measured by fitting Gaussian profiles through the stellar metallic lines using the IRAF *splot* task. There is no more than 15% difference among the equivalent widths of the same lines, measured in different spectra. We have excluded from our abundance determinations seriously

blended lines. The stellar lines were identified using the general references of *A multiplet table of astrophysical interest* (Moore 1945) and *Wavelengths and transition probabilities for atoms and atomic ions - Part 1: Wavelengths* (Reader et al. 1980), as well as more specialized reference for the Fe II lines (Johansson 1978). The final linelist is shown in a previous work (Saffe et al. 2008). In Figure 1 we present a comparison of our equivalent widths with those collected from literature, for 2 sample stars (HD 33636 and HD 82943). We compared our equivalent widths for 15 stars with those measured in the literature, and found a good agreement (dispersion $< \sim 5\%$).

3. Metallicity determinations using the WIDTH program

We have used the $uvby\beta$ mean colors of Hauck & Mermilliod (1998) with the calibration of Napiwotzki et al. (1993), to derive T_{eff} and $\log g$ using the TEMPLOGG code (Rogers et al. 1995). This program has been used in the COROT mission preparation (see, for example, Lastennet et al. 2001; Guillon & Magain 2006). The final values of the adopted T_{eff} and $\log g$ are listed in Table 1. With the chosen values of effective temperature and gravity, we computed a model atmosphere using Kurucz ATLAS9 (Kurucz 1992, 1993) code. Finally the Kurucz's model together with the measured equivalent widths are used by the WIDTH9 program (Kurucz 1992, 1993) to derive the metallicity.

For calculating the metallicity and microturbulent velocity we have used the standard method. We have computed abundances from Fe lines for a range of possible microturbulent velocities (ξ). For determining the final values, we looked for the condition that the abundances of FeI lines were not dependent on the equivalent widths. In this sense the abundance and microturbulent velocity determinations are simultaneous. Once a ξ value has been fixed, the corresponding abundances to all chemical species measured are determined using the WIDTH9 code. The final values of the metallicities are listed in Table 2.

To estimate errors for our WIDTH metallicities we consider the following facts. The most significant contribution to the final uncertainties comes usually from the equivalent width measurements. We assume a 5% error due to the continuum level determination. This translates into 20% maximum uncertainties in the metallicity estimation. The atomic constants may also have uncertainties. In particular we estimate that the oscillator strength values may cause differences of about 10% in the calculated metallicity. Finally to provide an estimation of "typical" errors introduced by the WIDTH method we increased the T_{eff} by 200 K and the $\log g$ by 0.20 dex, and recalculated the metallicity value for each star. We derived a median difference of 0.20 dex. The largest difference corresponds to HR 810 (0.48 dex).

4. Discussion of the results

4.1. Comparison of derived values with those from literature

Figure 2 shows the comparison of T_{eff} , $\log g$ and ξ obtained in this work, with those values from literature (R1,R2,...,R11). We mentioned that T_{eff} and $\log g$ were derived using Strömgren photometry with the Napiwotzki et al. (1993) calibration. In our derivation of [FeI/H] using the WIDTH9 program, the microturbulence velocity ξ is selected in order to have the abundances independent of the equivalent widths. Figure 2 shows that there is a good agreement of T_{eff} , $\log g$ and ξ with literature values.

¹ <http://exoplanets.org>

² <http://obswww.unige.ch/exoplanets>

³ On loan from the Institute d'Astrophysique de Liege, Belgium.

⁴ IRAF is distributed by the National Optical Astronomical Observatories which is operated by the Association of Universities for Research in Astronomy, Inc., under a cooperative agreement with the National Science Foundation.

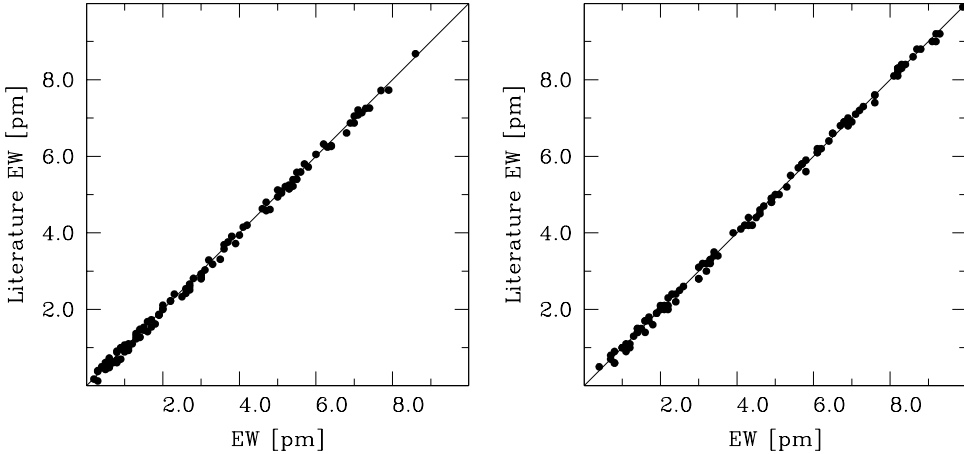


Fig. 1. Comparison of measured equivalent widths and from literature, for 2 sample stars (HD 33636 and HD 82943, left and right panels, respectively).

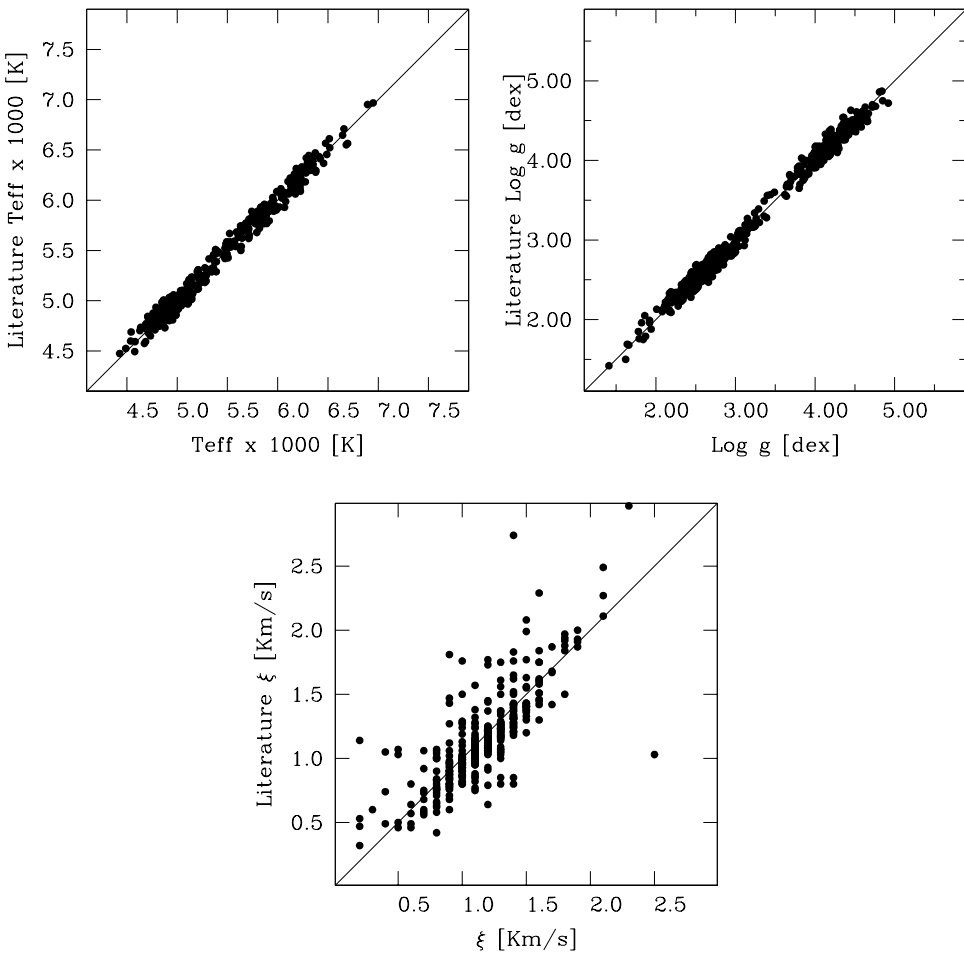


Fig. 2. Comparison of T_{eff} , $\log g$ and ξ obtained in this work, with those values from literature (R1,R2,...,R11).

Figure 3 shows the comparison of $[\text{Fe}/\text{H}]$ values derived using the WIDTH9 program, and $[\text{Fe}/\text{H}]$ from literature (using lines from both FeI and FeII). Upper panels present main sequence stars, showing EH stars and no-EH stars in the left and right panels, respectively. Lower panels present giant stars, showing EH stars and unknown EH stars in the left

and right panels, respectively. Main sequence $[\text{Fe}/\text{H}]$ values are from Nordström et al. (2004), and giant $[\text{Fe}/\text{H}]$ values from Takeda et al. (2008). There is a general agreement, although we notice two systematic tendencies: WIDTH9 values seem to be lower and slightly higher than literature, for main sequence and giant stars, respectively. We attribute this tendency to the differ-

ent calibrations and methods applied to derive the metallicity. A linear fit to the points of Figure 3, gives the following relations: $[Fe/H]_{WIDTH9} = 1.001[Fe/H]_{Literature} - 0.050$ dex, and $[Fe/H]_{WIDTH9} = 1.055[Fe/H]_{Literature} - 0.011$ dex, for main sequence and giants, respectively. We can use both relations to derive the metallicity values in the different scales.

4.2. The FeI and FeII layers

In this section we compare the layers in the atmosphere where FeI and FeII lines are formed. The WIDTH9 program provides an indication of the Rosseland median optical depth of formation for each line. We called this quantity τ_{FeI} and τ_{FeII} for FeI and FeII, respectively. We interpolated these values in the model atmosphere layers tabulated by ATLAS9 and estimated for τ_{FeI} and τ_{FeII} the temperature T, the electronic density n_e and molecular densities of the chemical species. We used a representative model for main sequence stars with $T_{eff} = 5800$ K, $\log g = 4.4$ dex, and a model for giant stars with $T_{eff} = 5000$ K, $\log g = 2.5$ dex, both with solar metallicity and $\xi = 2.0$ km/s. From the molecular densities in the ATLAS9 model, we derived the fraction FeI/FeII. We also computed this fraction assuming local thermodynamic equilibrium (LTE) and applying the Saha equation, using up to 9 ionization stages for the Fe. The partition functions values for FeI to FeX were obtained from Halenka & Madej (2002). We derived the electronic pressure P_e from $P_e = n_e k T$, where k is the Boltzmann constant and T is the temperature of the layer. We present in Table 1 the Rosseland median optical depth for the sample stars, the temperature T, and the FeII/FeI fraction (from ATLAS9 and our estimation), for the respective layers. We also present in the last two columns, the fraction of FeI atoms compared to the total number of Fe particles (neutral plus ionized), and the fraction of FeII ions to the same total. In this table we separated main sequence and giant stars, because the median values are different.

In this work we studied 4 groups of stars: main sequence EH and no-EH stars, giant EH and giant unknown-EH stars. From WIDTH9 and ATLAS9 data, τ_{FeI} and τ_{FeII} are indistinguishable for main sequence EH and no-EH stars. Then, we present in Table 1 the data for all main sequence stars (without separating EH and no-EH stars). For giant EH stars τ_{FeI} and τ_{FeII} are slightly different, while for giants unknown-EH $\tau_{FeI} \sim \tau_{FeII}$, as is shown in Table 1.

It is usually assumed that the atmosphere of the stars have a gradual mix of FeI, FeII and so on, in the layers with different T and P_e . From Table 1, main sequence stars (all), and giant EH stars, have different τ_{FeI} and τ_{FeII} , i.e. the median depth where the lines are formed. Only as a first order approximation, we could adopt $[FeI/H]$ and $[FeII/H]$ as an estimation of the Fe abundance at different depths τ_{FeI} and τ_{FeII} and $\Delta[Fe/H]$ as stratification indicator. Is desirable a longer depth difference than $\tau_{FeI} - \tau_{FeII}$ for an stratification study, using for example another chemical species or specific lines (this will be done in a future paper). Also, the FeII abundance was derived from a few number of lines (usually 3 lines, and only 1 line in some cases). Then, $\Delta[Fe/H]$ have a limited applicability as stratification indicator. However, the layers differ in temperature (~ 150 K) and electronic density, resulting in a different fraction of FeII/FeI at different optical depths. Taking into account the limitations, we consider that is a valid experiment to compare statistically both FeI and FeII abundances separately with another stellar or exoplanet parameters.

To solve the problem of the relatively short difference between τ_{FeI} and τ_{FeII} , we use another stratification indicator. We have computed the Rosseland median optical depth τ for each

FeI line using WIDTH9, and then derived the slope in a plot abundance vs. τ . We present in Figure 4 four examples of these relations. Each point in the plot correspond to a single FeI line in the stellar spectra. We adopt the slope of the plot (called Σ) as another stratification indicator, i.e. a non-stratified star would show a null Σ . For certain star, Σ represent the Fe gradient, evaluated at the median optical depth τ where the Fe lines are formed. In the next sections we will correlate these quantities with stellar and exoplanet parameters.

4.3. Correlations of $\Delta[Fe/H]$, τ and Σ with stellar parameters

The purpose of this section is to verify any correlation between $\Delta[Fe/H]$, τ and Σ with stellar parameters. If there is no relation at all, the comparison between EH and non-EH stars could be done by directly using $\Delta[Fe/H]$, τ and Σ on both groups. But, if there is any relation, the comparison between EH and non-EH stars should be done dividing the stars in subsamples with similar stellar parameters. We will explore this possibility in the next sections.

We have mentioned that $\Delta[Fe/H]$ have a limited use as stratification indicator. However, we search possible trends between $\Delta[Fe/H]$ and the stellar parameters. We find no obvious relation between $\Delta[Fe/H]$ and ξ , for main sequence and giant stars, with or without exoplanets. The large dispersion of values probably mask any relation between these parameters.

We present in Figure 5 the relation of τ_{FeI} (the Rosseland median optical depth of FeI lines), with the stellar parameters. For main sequence stars, we separated EH stars (filled circles) and no-EH stars (empty circles). For giant stars, we separated EH stars (filled circles) and unknown-EH stars (points). Notably, τ_{FeI} decreases with $\log g$ (all stars) and increases with ξ (giant stars). Also, τ_{FeI} decreases with T_{eff} (giant stars) and with $[FeI/H]$ (all stars). A similar relation is valid for τ_{FeII} vs. stellar parameters (not shown). We attribute these relations to the different physical conditions in the atmosphere of main sequence and giant stars. We do not find any obvious difference between EH and no-EH stars (or unknown-EH stars) in Figure 5.

Finally, we present in Figure 6 the plots of Σ with the stellar parameters. The symbols are the same of Figure 5. We do not find a clear relation for main sequence or giant stars, with or without exoplanets, in contrast to the trends mentioned for τ_{FeI} and τ_{FeII} . However, we caution that the dispersion of values in Figure 6 is very large.

4.4. Exoplanets vs. Solar Neighborhood

In this section we compare the stratification properties of stars with and without exoplanets. From Figure 5 we cannot discard the dependence of τ with the stellar parameters. Then, in order to compare $\Delta[Fe/H]$, τ and Σ for EH and non-EH stars, we have divided the sample of stars in subsamples with similar parameters. For main sequence stars, we have only 9 non-EH stars and 66 EH stars. Then, for each main sequence non-EH star, we search EH comparison stars with similar fundamental parameters, i.e. with differences up to 100 K, 0.2 dex, 0.2 dex and 0.1 km/s on T_{eff} , $\log g$, $[FeI/H]$ and ξ , respectively. On the other hand, for giant stars we have 13 EH stars and 313 non-EH stars. Then, for each giant EH star, we search non-EH stars with similar fundamental parameters. The values of the comparison groups are averaged, and presented in Tables 2 and 3, for main sequence and giant stars, respectively. Applying the cut criteria for the subsamples, 2 main sequence and 1 giant star resulted with empty subsamples.

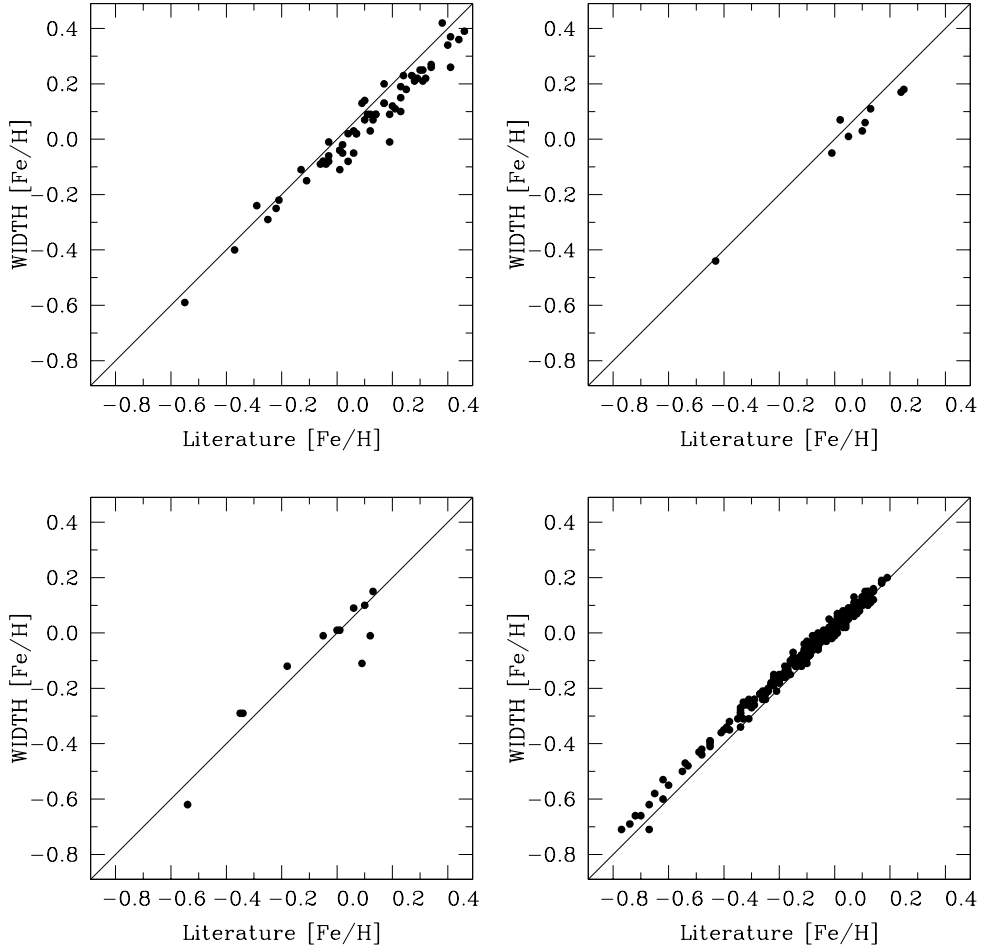


Fig. 3. Comparison of [FeI/H] values derived using the WIDTH9 program, and [Fe/H] from literature (using lines from both FeI and FeII). Upper panels present main sequence stars, showing EH stars and no-EH stars in the left and right panels, respectively. Lower panels present giant stars, showing EH stars and unknown EH stars in the left and right panels, respectively.

Table 1. Temperature, n_e and FeII/FeI at the layers with optical depth τ_{FeI} and τ_{FeII} .

Stars	τ	T [K]	n_e [cm $^{-3}$]	ATLAS9 FeII/FeI	Our FeII/FeI	Our FeI/Fe	Our FeII/Fe
Main sequence (all)	$\tau_{FeI} = 0.35$	5510	$1.25 \cdot 10^{13}$	16.0	13.9	0.93	$1.12 \cdot 10^{-7}$
	$\tau_{FeII} = 0.43$	5656	$1.61 \cdot 10^{13}$	19.5	17.3	0.95	$2.22 \cdot 10^{-7}$
Giant EH	$\tau_{FeI} = 0.98$	5443	$2.86 \cdot 10^{12}$	50.2	48.8	0.98	$3.32 \cdot 10^{-7}$
	$\tau_{FeII} = 1.22$	5682	$4.72 \cdot 10^{12}$	65.3	64.1	0.98	$9.23 \cdot 10^{-7}$
Giant unknown-EH	$\tau_{FeI} \sim \tau_{FeII} = 1.22$	5682	$4.72 \cdot 10^{12}$	65.3	64.1	0.98	$9.23 \cdot 10^{-7}$

Then, for these 3 stars (HD 10700, HD 149661 and HD 47536) we search the closest possible star in the stellar parameter space (HD 22049, HD 145675 and HD 36079, respectively).

From the values presented in the Tables 2 and 3, we conclude that $\Delta[\text{Fe}/\text{H}]$ and Σ are not statistically different for EH and non-EH stars (or unknown-EH stars). We do not find, for example, that most EH stars have Σ lower than non-EH stars. In particular, the main sequence star HD 75332 shows a high $\Delta[\text{Fe}/\text{H}]$ value (0.83 dex), based only in 1 FeII line. We already mentioned the limited use of $\Delta[\text{Fe}/\text{H}]$ as stratification indicator.

The fact that Σ is not statistically different for EH and non-EH stars (or unknown-EH stars), is in agreement with the primordial hypothesis of metal enhancement. If the accretion hypothesis is true for EH stars, the external layers are initially metal-rich while the more internal layers should maintain the lower original metal content. Then, for giant stars the very deep convective zone should mix the layers of the atmosphere, returning the upper layers to the original metal-poor values. A similar process could work in main sequence stars, but now the CZ is smaller than the CZ of a giant star, and the metal increase in the upper layers should be evident, resulting in a stratified atmo-

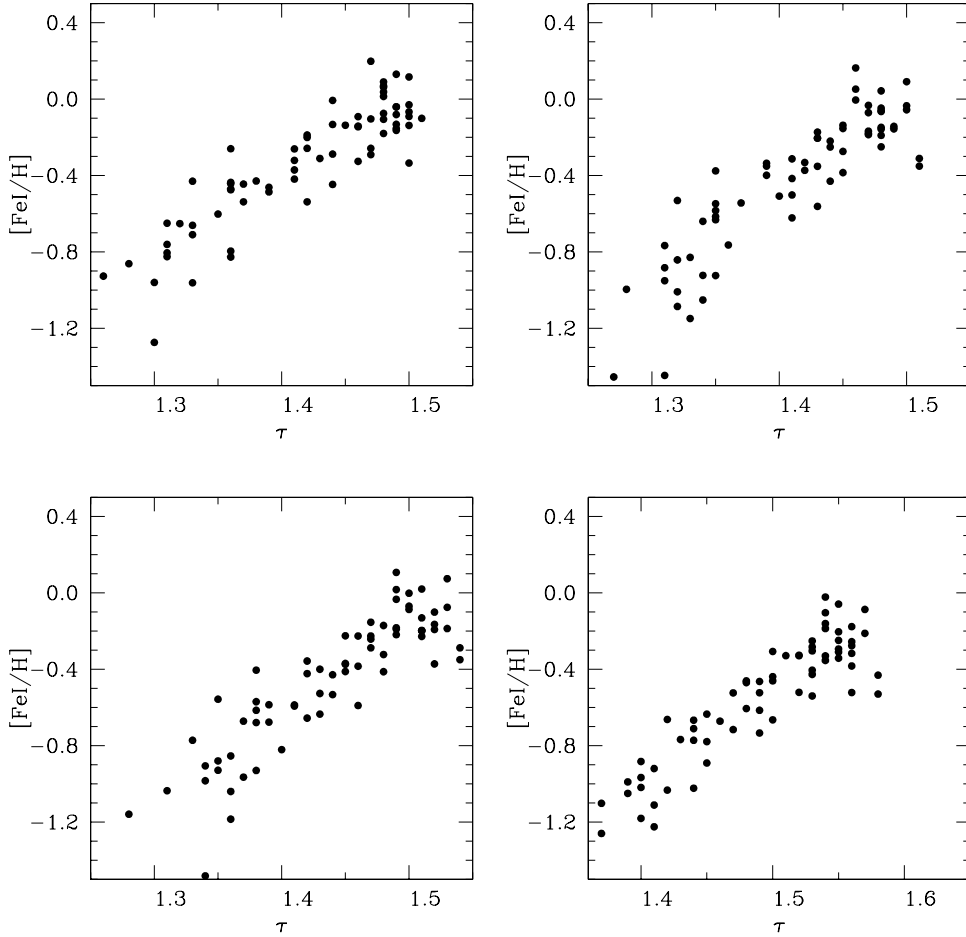


Fig. 4. Four examples of $[\text{FeI}/\text{H}]$ vs. τ_{FeI} : HD 107950 and HD 83805 (upper panels), HD 91190 and HD 91612 (lower panels).

sphere. If we use Σ as stratification indicator (and $\Delta[\text{Fe}/\text{H}]$ also), the Tables 2 and 3 indicate that EH and non-EH stars present a similar stratification structure, at the median optical depth where the Fe lines are formed. Then, the accretion hypothesis of metal-excess in EH stars is less favored, however this do not discard completely the possibility that some EH stars could suffer an accretion process.

Some stars in Tables 2 and 3 have indications of possible stratification. For example, 4 stars in the Table 3 (HD 47536, HD 137759, HD 219449 and HD 199665) present $\Sigma < 0$ and significantly different from Σ of their respective comparison subsample stars. We consider that these 4 stars are candidates to have an stratified atmosphere. We also derived the number of stars with $\Sigma < 0$: 20% (13/65) main sequence EH stars and 33% (4/12) giant EH stars. Giant stars present a higher percentage of stratified stars than main sequence stars. This is relatively surprising because giant stars are supposed to have larger CZs than main sequence stars. However, the difference could probably due the fact that giant stars have stellar radius 10-20 times larger than main sequence stars, then the external contamination of the photosphere seems to be more probable. We caution that the number of stars used to derive these fractions are too low, particularly for giant stars, and more stars are needed to confirm this initial trend.

To complement the analysis, we also show the entire distribution of values (without subsampling). We caution that this comparison have the bias of the stellar parameters, particularly

for τ_{FeI} and τ_{FeII} as we showed in the previous sections. We present in Figure 7 (upper panels) the distribution of $\Delta[\text{Fe}/\text{H}]$ values, for EH stars, non-EH stars and unknown-EH stars. Main sequence and giant stars are presented in left and right panels, respectively. The plot show that EH stars and no-EH stars have a similar distribution of $\Delta[\text{Fe}/\text{H}]$ values, and this is valid for main sequence and giant stars separately. A Kolmogorov-Smirnov (KS) test derive a possibility of 68% and 83% that both samples represent the same population, for main sequence and giant stars, respectively. We note that the range in $\Delta[\text{Fe}/\text{H}]$ is larger for giants than main sequence stars. This is probably due to the larger number of lines used to derive $\Delta[\text{Fe}/\text{H}]$ in the giants, compared with main sequence stars.

The central panels of Figure 7 shows the distribution of the optical depth τ_{FeI} , using the same symbols of the upper panels. Main sequence stars present a similar distribution of values (EH and non-EH stars). On the other hand, giant stars show a different behaviour (EH and unknown-EH). A KS test derive a possibility of 38% and 35%, that both samples represent the same population, for main sequence and giant stars, respectively. The apparent peak for EH giant stars with $\tau_{\text{FeI}} < 0.8$ is composed only by 3 stars: HD 192091, HD 167042 and HD 137759. The next bin is composed by 2 stars: HD 219449 and HD 210277. From these 5 stars, 3 of them (HD 192091, HD 167042 and HD 210702) have large $\log g$ values compared to other giants in our sample (3.21, 3.28 and 3.19 dex, respectively), and relatively small ξ values (0.9, 0.9 and 1.0 km/s, respectively). The large $\log g$

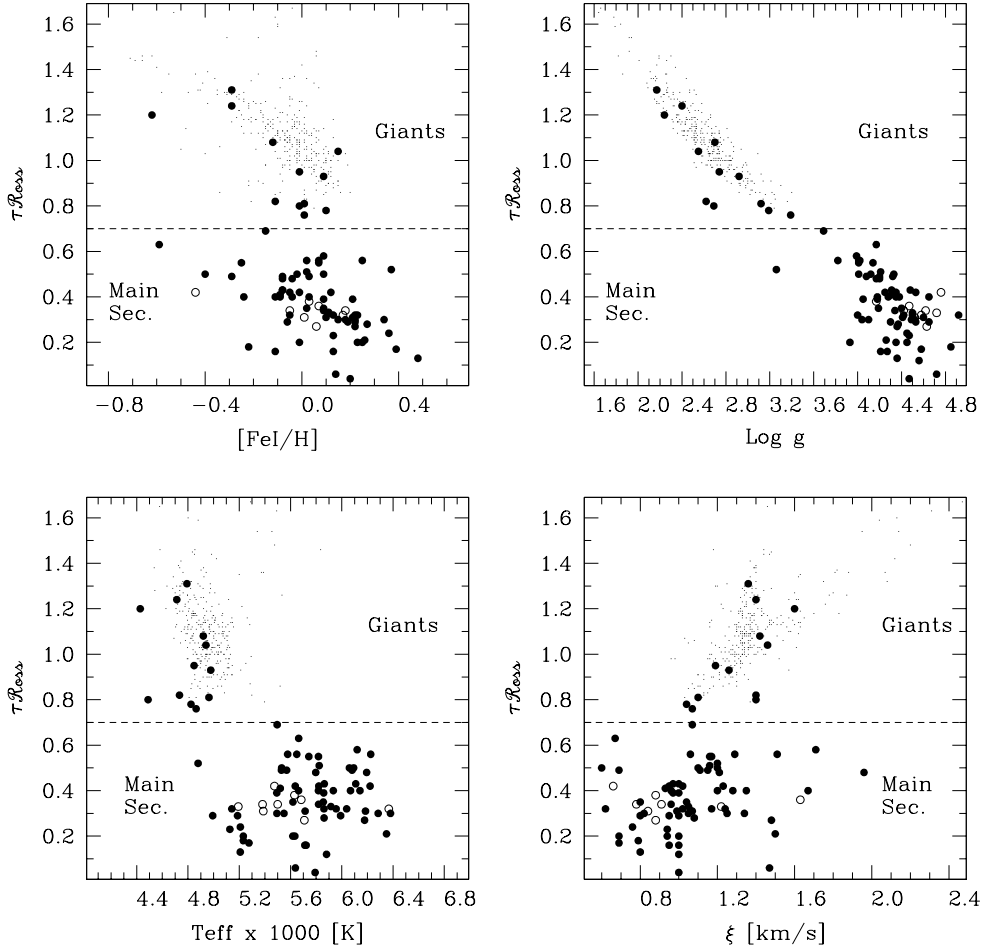


Fig. 5. Correlations of τ_{FeI} with stellar parameters. We separated main sequence stars (EH stars with filled circles and no-EH stars with empty circles) and giant stars (EH stars with filled circles and unknown-EH stars with points).

and small ξ values, both produce a bias in favor of smaller τ_{FeI} values. Then, the apparent peak in the distribution of τ_{FeI} values seems to be unreal (or, it have the bias of stellar parameters). The proper comparison of τ_{FeI} values should be done separating in subsamples, as presented in Tables 2 and 3.

Lower panels of Figure 7 shows the distribution of Σ , using the same symbols. Again, main sequence stars shows a similar distribution of values for EH and non-EH stars, while EH giant stars seem to have a peak at $\Sigma < -0.02$. Σ is less dependent on stellar parameters than τ_{FeI} and then the peak could be real. The apparent peak is composed only by 3 stars: HD 47536, HD 137759 and HD 219449. We previously mentioned that these 3 stars have very low Σ values compared to a subsample of stars with similar fundamental parameters. We note that HD 47536 is an extremely metal-poor giant star ($[FeI/H] = -0.62$). If we exclude these 3 stars, the distributions are very similar. Then, we can conclude that the distributions of Σ for giants EH and unknown-EH are similar, except probably for some EH giant stars that show $\Sigma < -0.02$. The comparison do not have strong statistical significance, because we are comparing two distributions, one of them with a few number of points. Then, this result is only an initial trend to be confirmed.

5. Stratification vs. Exoplanet Parameters

The values of $\Delta[Fe/H]$, τ and Σ could be also compared to the exoplanet parameters, such as minimum mass $M \sin i$, eccentricity and semiaxis. $\Delta[Fe/H]$ is based usually in a reduced number of FeII lines, and we showed in the previous sections that τ_{FeI} and τ_{FeII} depend strongly on stellar parameters, particularly on $\log g$. Σ is less dependent on stellar parameters and is derived from a number of FeI lines. Then, we adopt Σ as a more reliable stratification indicator to compare with the Exoplanet parameters. We present in the Figure 8 a plot of Σ vs. the exoplanet parameters, for the sample of EH stars. Main sequence EH stars are presented with filled circles, and giant EH stars with empty circles. There is no clear relation.

In the accretion hypothesis, the bombardment of EH stars by metal-rich planetesimals result in a metallicity increase of the upper layers of the atmospheres and also probably stratified atmospheres. We can expect that both effects are more easily observable in main sequence than giant stars, because the larger CZ in giant stars would mix layers with low and high metal content. Then, we could use the stratification data and the exoplanet parameters to test the accretion hypothesis, at least in main sequence stars. For example, we could admit that the accretion (and also stratification) is more probable to occur for those exoplanets closer to the stars, or exoplanets in very eccentric orbits, or with the more massive planets. The existence of such

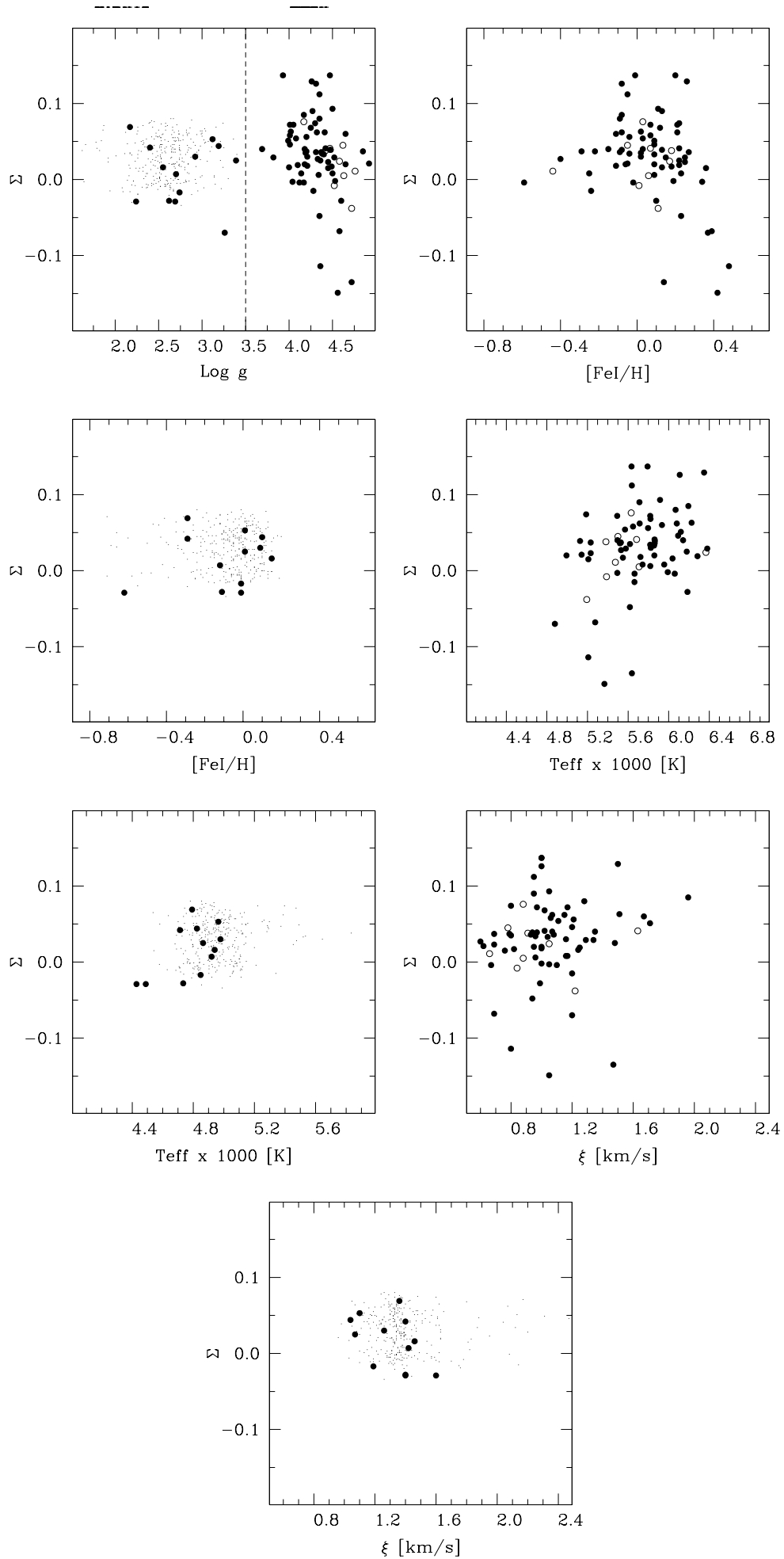


Table 2. Main sequence non-EH stars, and EH subsamples of stars for comparison.

Star	τ_{FeI}	τ_{FeII}	$\Delta[Fe/H]$	Σ	n_1	n_2
HD 75332	0.32	0.38	0.83	0.024	12	1
7 comparison stars	0.28	0.37	-0.01	0.050		
16 Cyg A	0.38	0.45	-0.07	0.076	22	3
8 comparison stars	0.39	0.43	0.02	0.034		
HD 10700	0.42	0.46	0.07	0.011	126	3
1 comparison star	0.29	0.59	0.05	0.020		
HD 17925	0.33	0.40	0.12	-0.038	92	3
4 comparison stars	0.24	0.41	-0.02	-0.024		
HD 69830	0.34	0.49	0.02	0.045	110	5
7 comparison stars	0.36	0.45	-0.03	0.025		
HD 76151	0.36	0.41	0.05	0.041	116	7
13 comparison stars	0.32	0.41	0.00	0.037		
HD 104304	0.34	0.46	0.03	0.038	115	6
12 comparison stars	0.33	0.41	0.00	0.037		
HD 115617	0.27	0.33	0.06	0.005	110	3
2 comparison stars	0.30	0.53	0.00	0.021		
HD 149661	0.31	0.39	0.08	-0.008	112	2
1 comparison star	0.24	0.41	0.03	0.015		

Table 3. Giant EH stars, and solar neighborhood subsamples for comparison.

Star	τ_{FeI}	τ_{FeII}	$\Delta[Fe/H]$	Σ	n_1	n_2
HD 47536	1.20	1.55	-0.05	-0.029	31	3
1 comparison star	1.24	1.44	0.02	0.037		
HD 137759	0.80	1.30	-0.06	-0.029	26	3
50 comparison stars	1.10	1.24	0.01	0.036		
HD 219449	0.82	1.26	-0.04	-0.028	29	3
23 comparison stars	1.15	1.31	0.00	0.039		
HD 28305	1.04	1.21	0.01	0.016	66	3
74 comparison stars	1.06	1.20	0.03	0.028		
HD 62509.2	0.93	1.14	0.03	0.030	76	3
83 comparison stars	0.98	1.13	0.02	0.029		
HD 81688	1.31	1.46	-0.03	0.069	70	3
34 comparison stars	1.27	1.37	0.01	0.030		
HD 104985	1.24	1.32	0.03	0.042	67	2
63 comparison stars	1.21	1.32	0.01	0.031		
HD 142091	0.78	1.03	0.00	0.044	75	3
10 comparison stars	0.85	1.03	0.03	0.038		
HD 167042	0.76	1.00	0.07	0.025	77	3
11 comparison stars	0.86	1.02	0.01	0.029		
HD 188310	1.08	1.25	0.05	0.007	71	2
111 comparison stars	1.06	1.20	0.02	0.032		
HD 199665	0.95	1.11	0.00	-0.017	72	3
42 comparison stars	0.98	1.12	0.02	0.021		
HD 210702	0.81	1.03	0.01	0.053	78	3
14 comparison stars	0.87	1.02	0.02	0.034		

correlation, for example between Σ and EH stars with the closer exoplanets, would be in agreement with the accretion hypothesis. Then, the lack of correlation between Σ and the exoplanet parameters (a , e , $M \sin i$) favors the primordial hypothesis of metal-enrichment rather than the accretion. However, this lack of correlation do not completely rule out possible accretion events in some EH stars.

Another possible test of the accretion hypothesis uses the values of Σ and [FeI/H]. Such stars that suffered an important accretion, would result in an increase of [FeI/H] and also probably a decrease in Σ . Then, we could expect a relation between [FeI/H] and Σ for accreted stars. We do not see any trend between [FeI/H] and Σ for most of the EH stars (see Figure 6), then the primordial hypothesis is favored. Again, this do not rule out the accretion in some EH stars. We can divide the plot [FeI/H] vs. Σ

in two regions: stars with $\Sigma < 0$ and with $\Sigma > 0$. The first region would correspond to candidate stars with stratified atmospheres, because they have precisely $\Sigma < 0$. In this region, the stars seem to present a relation in which Σ decreases with [FeI/H], i.e. a relation expected for stars with accretion. For these stars the stratification could be related to the accretion.

6. The metal-rich nature of EH stars

As we explained in the introduction, it is well established that main sequence EH stars with giant planets are, on average, metal-rich in comparison to stars that do not harbor Doppler-detected planets (see, for example, Santos et al. 2004). On the other hand, for giant EH stars there are different trends in the literature. Pasquini et al. (2007) derived solar metallicities for a group of 14 giant EH stars. Hekker & Meléndez (2007) do not

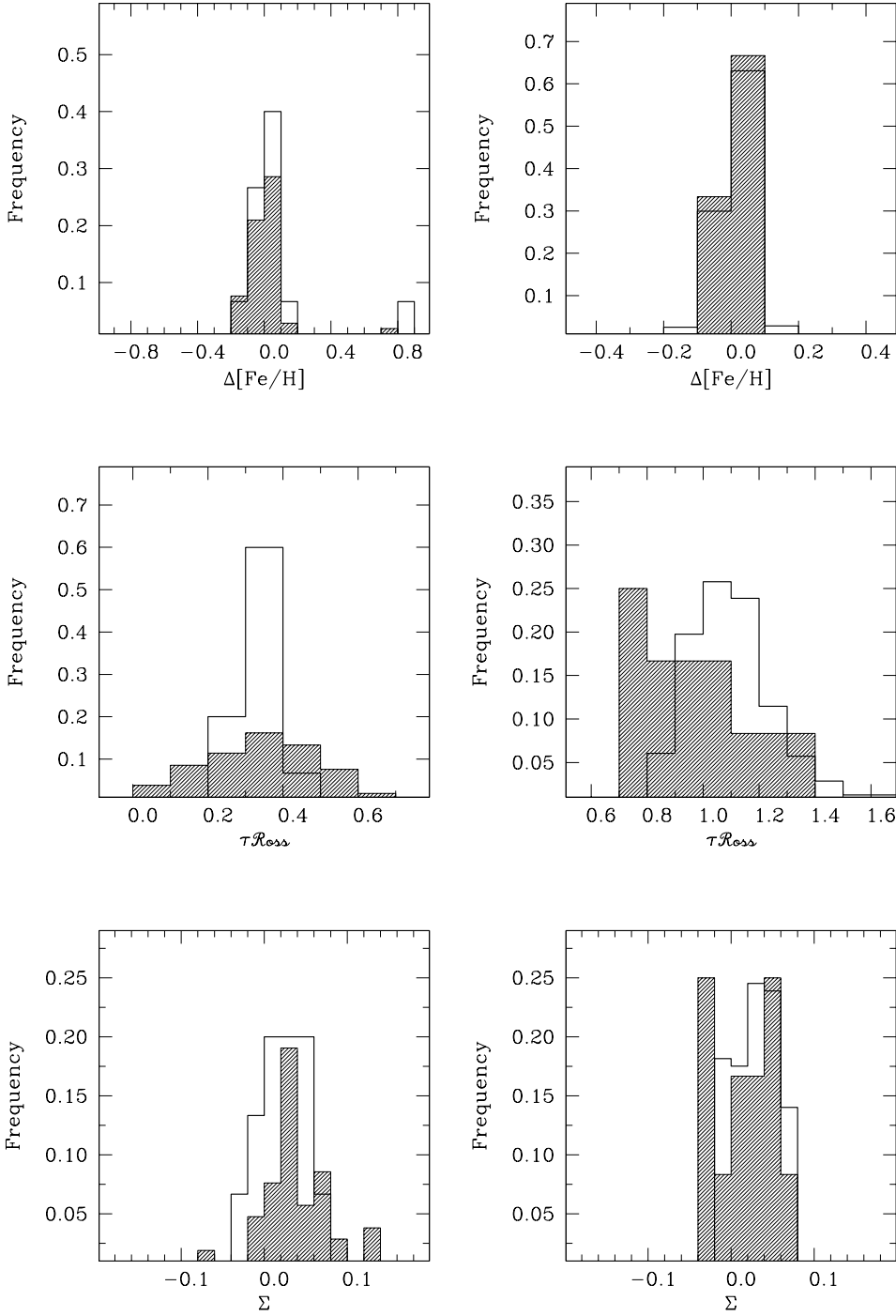


Fig. 7. EH stars vs. solar neighborhood stars: distribution of $\Delta[\text{Fe}/\text{H}]$ values (upper panels), $\tau_{\text{Fe}I}$ (central panels) and Σ (lower panels).

confirm Pasquini et al.'s result, based on 20 objects. The metallicity of giant EH stars is not well understood, probably due to the reduced number of stars studied.

Our sample of stars include 13 giant EH stars, and 313 giant unknown-EH stars. The metallicity distribution of these samples is presented in Figure 9. From the plot, giant EH stars seems to have a similar metallicity distribution compared with giant unknown-EH stars. The KS test result in a probability of 52% that both distributions represent the same statistical population.

Certainly, giant unknown-EH stars could be contaminated by a group of EH stars. However, the data presented in this work suggest that there is a number of giant EH stars with solar metallicity values (median of -0.09 dex). Our result is in agreement with Pasquini et al. (2007) rather than Hekker & Meléndez (2007). We caution that the number of giant EH stars studied is still small and more stars are needed to verify this initial trend.

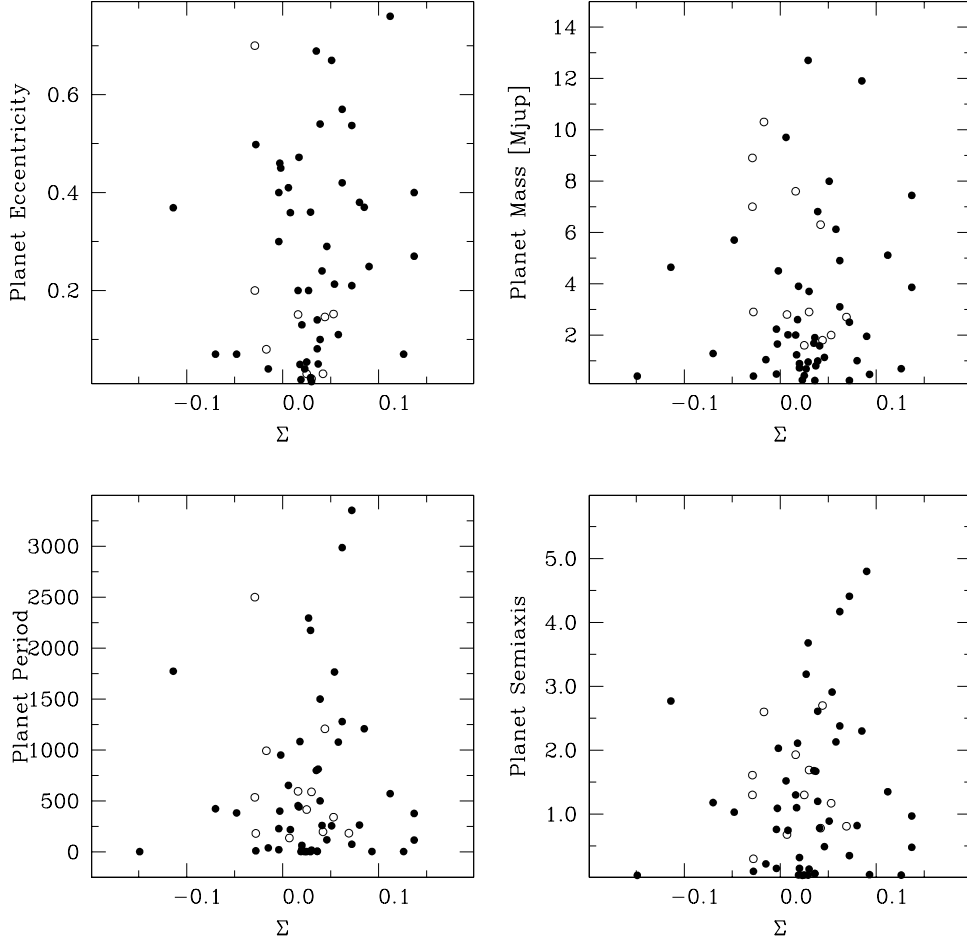


Fig. 8. Stratification (Σ) vs. exoplanet parameters in EH stars. Main sequence EH stars are presented with filled circles, and giant EH stars with empty circles.

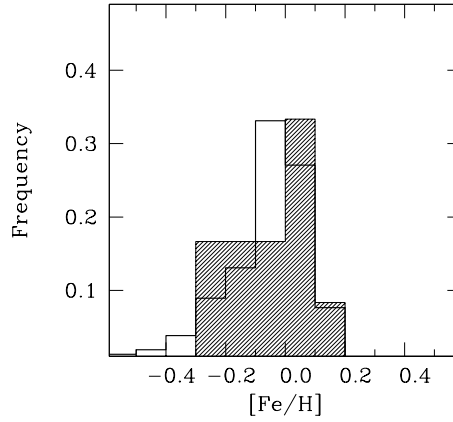


Fig. 9. Metallicity distribution of giant EH stars and unknown-EH stars.

7. Summary and Conclusions

The Rosseland median optical depth τ_{FeI} and τ_{FeII} are dependent on stellar parameters ($\log g$, T_{eff} and ξ). We conclude that Σ is more reliable stratification indicator than τ_{FeI} , τ_{FeII} and $\Delta[\text{Fe}/\text{H}]$. Our results show that statistically most EH stars (main sequence and giants) have an stratification similar to field stars,

which is in agreement with the primordial hypothesis of metal enhancement. The lack of correlation between Σ and the exoplanet parameters (minimum mass, semimajor axis and eccentricity) for most of the EH stars, and between $[\text{Fe}/\text{H}]$ and Σ , favors the primordial hypothesis of metal-enrichment. However, we cannot discard that some EH stars (and even non-EH stars) have

suffered and accretion process in the past. We consider candidate stars with stratified atmospheres those with $\Sigma < 0$ (7 main sequence stars and 4 giant stars). The group of candidate EH main sequence stars with stratified atmospheres ($\Sigma < 0$), seems to show a correlation with [Fe/H], which probably relate the stratification in these stars with accretion events.

Acknowledgements. The authors thank Drs. F. Castelli, P. Bonifacio and L. Sbordone for making their codes available to them.

References

- González, G., 1998, A&A 334, 221
 González, G., 2006, PASP 118, 1494
 González, G., Laws, C., 2000, AJ 119, 390
 González, G., Laws, C., Tyagi, S., Reddy, B. E., 2001, AJ 121, 432
 González, G., Wallerstein, G., Saar, S., 1999, ApJ 511, 111
 Gillon, M., & Magain, P. 2006, A&A, 448, 341
 Halenka, J., Madej, J., 2002, Acta Astronomica 52, 199
 Hauck, B., & Mermilliod, M. 1998, A&AS, 129, 431
 Hekker, S., Meléndez, J. 2007, A&A, 475, 1003
 Johansson S. 1978, Phys. Scripta, 18, 217
 Kurucz, R. L. 1992, Rev. Mexicana Astron. Astrofis., 23, 45
 Kurucz, R. L. 1993, ATLAS) *Stellar Atmosphere Programs and 2 km/s grid*, Kurucz CM-ROM No. 13, Smithsonian Astrophysical Observatory, Cambridge, MA
 Lastennet, E., Lignies, F., Buser, R., Lejeune, T., Lftinger, T., Cuisinier, F., & van't Veer-Mennenet, C. 2001, The Journal of Astronomical Data Vol. 7
 Laws, C., González, G., 2001, ApJ 553, 405
 Laws, C., González, G., Walker, K. M., Tyagi, S., Dodsworth, J., Snider, K., Suntzeff, N. B., 2003, AJ 125, 2664
 Moore, C. E. 1945, *A multiplet table of astrophysical interest* Princeton, N.J., The Observatory, 1945. Rev. ed.
 Napiwotzki, R., Schoenberner, D., & Wenske, V. 1993, A&A, 268, 653
 Nordström, B., Mayor, M., Andersen, J., Holmberg, J., Pont, F., Jorgensen, B. R., Olsen, E. H., Udry, S., & Mowlavi, N. 2004, A&A, 418, 989
 Pasquini, L., Döllinger, M. P., Weiss, A., Girardi, L., Chavero, C., Hatzes, A. P., da Silva, L., & Setiawan, J. 2007, A&A, 473, 979
 Reader, J., Corliss, C. H., Wiese, W. L., & Martin, G. A. 1980, *Wavelengths and transition probabilities for atoms and atomic ions - Part I: Wavelengths* National Standard Reference Data Series (NSRDS-NBS), Washington: National Bureau of Standards (NBS)
 Rogers, N. Y. 1995, Comm. in Asteroseismology 78
 Sadakane, K., Ohnishi, T., Ohkubo, M., Takeda, Y., 2005, PASJ 57, 127
 Saffe, C., Gomez, M., Pintado, O., Gonzalez, E., 2008, A&A 490, 297
 Saffe, C., Levato, H., López-García, Z., RMxAA 41, 415
 Saffe, C., Levato, H., López-García, Z., RMxAA 40, 231
 Santos, N. C., Israeliian, G., Mayor, M., 2000, AA 363, 228
 Santos, N. C., Israeliian, G., & Mayor, M. 2001, A&A, 373, 1019
 Santos, N. C., Israeliian, G., & Mayor, M. 2004, A&A, 415, 1153
 Santos, N. C., Israeliian, G., Mayor, M., Bento, J. P., Almeida, P. C., Sousa, S. G., Ecuivillon, A., 2005, A&A, 437, 1127
 Sousa, S. G., Santos, N. C., Mayor, M., Udry, S., Casagrande, L., Israeliian, G., Pepe, F., Queloz, D., & Monteiro, M. J. P. F. G. 2008, A&A, in press
 Takeda, Y., Ohkubo, M., Sato, B., Kambe, E., Sadakane, K., 2005, PASJ 57, 27
 Takeda, Y., Sato, B., Murata, D., 2008, PASJ 60, 781
 Udry, S., Mayor, M., Benz, W., Bertaux, J. L., Bouchy, F., Lovis, C., Mordasini, C., Pepe, F., Queloz, D., & Sivan, J. P. 2006, A&A, 447, 361
 Zhao, G., Chen, Y.-Q., Qiu, H.-M., 2002, ChJAA 4, 377

Table 1. Sample stars studied in this work and the correponding source of equivalent widths.

Star	T _{eff} [K]	log g [dex]	Exoplanet Host	Giant Star	Equivalent Width Ref.
rho crb	5663	4.28	yes	no	R1
47 Uma = HR 4277	5722	4.21	yes	no	R1
70 Vir = HR 5072	5634	3.93	yes	no	R1
HD 114762	5881	4.56	yes	no	R1
14 her = GJ 614	5208	4.36	yes	no	R2
HD 75289	6178	4.36	yes	no	This Work
nu and	6142	4.18	yes	no	R3
tau boo	6284	4.10	yes	no	R3
rho cnc	5187	4.30	yes	no	R3
HD 75332	6367	4.58	no	no	R4
HD 130322	5433	4.36	yes	no	This Work
HD 192263	4993	4.65	yes	no	R4
HD 209458	6109	4.31	yes	no	R4
51 Peg = HR 8729	5915	4.50	yes	no	R4
HD 222582	5637	4.35	yes	no	This Work
HR 810	6221	4.53	yes	no	R4
HD 177830	4678	3.42	yes	no	R4
BD -10 3166	5408	4.30	yes	no	R4
16 cyg A = HR 750	5631	4.17	no	no	R5
16 cyg B = HR 750	5619	4.19	yes	no	R5
HD 47536	4428	2.24	yes	yes	R6
HD 59686	4674	2.54	no	yes	R6
HD 137759	4489	2.69	yes	yes	R6
HD 219449	4734	2.62	yes	yes	R6
HD 1237	5638	4.72	yes	no	This Work
HD 13445	5232	4.85	yes	no	R7
HD 83443	5367	4.56	yes	no	This Work
HD 4203	5494	4.04	yes	no	R8
HD 4208	5529	4.20	yes	no	This Work
HD 6434	5664	4.17	yes	no	This Work
HD 8574	6060	4.12	yes	no	R8
HD 28185	5618	4.35	yes	no	This Work
HD 37124	5531	4.33	yes	no	R8
HD 46375	5232	4.45	yes	no	R8
HD 68988	5862	4.37	yes	no	R8
HD 106252	5864	4.48	yes	no	R8
HD 114783	5127	4.47	yes	no	This Work
HD 136118	6194	4.17	yes	no	R8
HD 141937	5819	4.34	yes	no	This Work
HD 168746	5520	4.31	yes	no	This Work
HD 202206	5704	4.38	bd	no	This Work
HD 27442	4879	3.26	yes	no	This Work
HD 108147	6185	4.60	yes	no	This Work
HD 121504	5859	4.18	yes	no	This Work
HD 160691	5714	4.41	yes	no	This Work
HD 213240	5991	4.53	yes	no	This Work
HD 12661	5632	4.13	yes	no	R9
HD 19994	6038	4.00	yes	no	This Work
HD 29587	5532	4.33	bd	no	R9
HD 92788	5792	4.47	yes	no	This Work
HD 98230	5852	4.42	bd	no	R9
HD 120136	6349	4.26	yes	no	R9
HD 187123	5712	4.27	yes	no	R9
HD 190228	5276	3.64	bd	no	R9
HD 123	5805	4.84	unkn	no	R10
HD 400	6221	4.05	unkn	no	R10
HD 693	6170	4.19	unkn	no	R10
HD 4307	5612	3.85	unkn	no	R10
HD 4614	5891	4.54	unkn	no	R10

Table 1. Continued.

Star	T _{eff} [K]	log g [dex]	Exoplanet Host	Giant Star	Equivalent Width Ref.
HD 4628	5041	4.60	unkn	no	R10
HD 4813	6281	4.51	unkn	no	R10
HD 5015	6129	3.99	unkn	no	R10
HD 6582	5360	4.60	unkn	no	R10
HD 6920	5951	3.87	unkn	no	R10
HD 7439	6348	4.07	unkn	no	R10
HD 7476	6457	3.69	unkn	no	R10
HD 9562	5871	4.21	unkn	no	R10
HD 9826	6226	4.02	yes	no	R10
HD 10307	5961	4.34	unkn	no	R10
HD 10476	5288	4.50	unkn	no	R10
HD 10697	5649	4.01	yes	no	R10
HD 10700	5475	4.76	no	no	R10
HD 10780	5507	4.45	unkn	no	R10
HD 13555	6425	3.99	unkn	no	R10
HD 14214	6176	4.07	unkn	no	R10
HD 15335	5883	3.74	unkn	no	R10
HD 15798	6189	3.81	unkn	no	R10
HD 16141	5818	4.01	yes	no	R10
HD 16673	6302	4.52	unkn	no	R10
HD 16895	6292	4.23	unkn	no	R10
HD 17925	5193	4.72	no	no	R10
HD 18803	5606	4.36	unkn	no	R10
HD 20630	5892	4.36	unkn	no	R10
HD 21019	5390	3.68	unkn	no	R10
HD 22049	5142	4.92	yes	no	R10
HD 22484	6041	3.99	unkn	no	R10
HD 30562	5894	4.10	unkn	no	R10
HD 30743	6186	3.82	unkn	no	R10
HD 32923	5718	3.80	unkn	no	R10
HD 33636	5934	4.65	yes	no	This Work
HD 34411	5742	4.17	unkn	no	R10
HD 35296	6169	4.36	unkn	no	R10
HD 38529	5578	3.82	yes	no	This Work
HD 39587	5924	4.54	unkn	no	R10
HD 43042	6477	4.35	unkn	no	R10
HD 43318	6119	3.82	unkn	no	R10
HD 49933	6518	3.88	unkn	no	R10
HD 50554	6080	4.32	yes	no	R10
HD 52265	6093	4.01	yes	no	This Work
HD 52711	5910	4.39	unkn	no	R10
HD 55575	5884	4.38	unkn	no	R10
HD 59984	5953	4.07	unkn	no	R10
HD 61421	6514	4.11	unkn	no	R10
HD 67228	5836	3.78	unkn	no	R10
HD 67767	5153	3.44	unkn	no	R10
HD 69830	5500	4.62	no	no	R10
HD 69897	6103	4.16	unkn	no	R10
HD 70110	5868	3.95	unkn	no	R10
HD 75732	5276	4.58	yes	no	R10
HD 76151	5684	4.47	no	no	R10
HD 76932	5772	4.10	unkn	no	R10
HD 79028	5955	3.94	unkn	no	R10
HD 81809	5712	3.84	unkn	no	R10
HD 82328	6162	3.80	unkn	no	R10
HD 82885	5586	4.48	unkn	no	R10
HD 82943	5956	4.50	yes	no	This Work
HD 84737	5957	4.17	unkn	no	R10
HD 86728	5813	4.58	unkn	no	R10
HD 87141	6310	3.78	unkn	no	R10

Table 1. Continued.

Star	T _{eff} [K]	log g [dex]	Exoplanet Host	Giant Star	Equivalent Width Ref.
HD 88737	6244	3.68	unkn	no	R10
HD 88986	5769	4.27	unkn	no	R10
HD 89125	6131	4.06	unkn	no	R10
HD 89744	6120	3.99	yes	no	R10
HD 91752	6659	4.48	unkn	no	R10
HD 91889	5997	4.05	unkn	no	R10
HD 95128	5797	4.20	yes	no	R10
HD 95241	5988	3.65	unkn	no	R10
HD 98991	6344	3.29	unkn	no	R10
HD 99491	5360	4.20	unkn	no	R10
HD 99747	6950	4.51	unkn	no	R10
HD 101501	5501	4.54	unkn	no	R10
HD 102634	6319	4.29	unkn	no	R10
HD 102870	6145	4.15	unkn	no	R10
HD 103095	5181	4.69	unkn	no	R10
HD 104304	5382	4.42	no	no	R10
HD 107213	6238	4.07	unkn	no	R10
HD 109358	5875	4.32	unkn	no	R10
HD 110897	5845	4.40	unkn	no	R10
HD 111395	5609	4.43	unkn	no	R10
HD 114642	6412	3.90	unkn	no	R10
HD 114710	6223	4.66	unkn	no	R10
HD 114946	5002	3.14	unkn	no	R10
HD 115383	6201	4.20	unkn	no	R10
HD 115617	5708	4.63	no	no	R10
HD 117176	5496	3.69	yes	no	R10
HD 121370	6329	4.01	unkn	no	R10
HD 122742	5414	4.15	unkn	no	R10
HD 124570	6132	3.92	unkn	no	R10
HD 124850	6296	4.05	unkn	no	R10
HD 125184	5714	4.05	unkn	no	R10
HD 127334	5590	4.42	unkn	no	R10
HD 128167	6894	4.51	unkn	no	R10
HD 131156	5482	4.54	unkn	no	R10
HD 131511	5200	4.58	unkn	no	R10
HD 134987	5861	4.42	yes	no	This Work
HD 136064	6214	3.83	unkn	no	R10
HD 137052	6646	4.06	unkn	no	R10
HD 137108	5889	4.19	unkn	no	R10
HD 137510	6152	4.30	unkn	no	R10
HD 141004	5827	4.08	unkn	no	R10
HD 142373	5712	3.84	unkn	no	R10
HD 142860	6247	3.96	unkn	no	R10
HD 143761	5743	4.14	yes	no	R10
HD 144585	5773	4.00	unkn	no	R10
HD 145675	5209	4.45	yes	no	R10
HD 149661	5388	4.52	no	no	R10
HD 150706	6068	4.35	yes	no	R10
HD 151769	6124	3.36	unkn	no	R10
HD 153597	6239	4.50	unkn	no	R10
HD 156826	5207	3.64	unkn	no	R10
HD 157214	5649	4.28	unkn	no	R10
HD 161797	5566	4.03	unkn	no	R10
HD 163989	6166	3.95	unkn	no	R10
HD 165341	5335	4.47	unkn	no	R10
HD 165908	6275	4.42	unkn	no	R10
HD 168009	5811	4.47	unkn	no	R10
HD 168151	6682	4.26	unkn	no	R10
HD 168443	5570	4.08	yes	no	This Work
HD 169830	6330	4.13	unkn	no	This Work

Table 1. Continued.

Star	T _{eff} [K]	log g [dex]	Exoplanet Host	Giant Star	Equivalent Width Ref.
HD 173667	6696	4.14	unkn	no	R10
HD 178428	5616	4.18	unkn	no	R10
HD 179949	6380	4.52	yes	no	This Work
HD 181096	6215	3.96	unkn	no	R10
HD 181655	5706	4.61	unkn	no	R10
HD 182488	5317	4.64	unkn	no	R10
HD 182572	5485	4.03	unkn	no	R10
HD 185144	5344	4.67	unkn	no	R10
HD 186408	5782	4.23	unkn	no	R10
HD 186427	5856	4.40	yes	no	R10
HD 187013	6489	4.15	unkn	no	R10
HD 187691	6066	4.08	unkn	no	R10
HD 190406	5976	4.35	unkn	no	R10
HD 193664	6016	4.53	unkn	no	R10
HD 195019	5824	4.21	yes	no	R10
HD 196755	5684	3.92	unkn	no	R10
HD 197076	5727	4.52	unkn	no	R10
HD 199960	5829	4.31	unkn	no	R10
HD 200790	6032	3.96	unkn	no	R10
HD 207978	6374	4.07	unkn	no	R10
HD 210277	5549	4.49	yes	no	This Work
HD 210855	6174	3.62	unkn	no	R10
HD 215648	6231	3.86	unkn	no	R10
HD 216385	6155	3.82	unkn	no	R10
HD 217014	5821	4.25	yes	no	R10
HD 217107	5493	4.05	yes	no	This Work
HD 218470	6336	3.98	unkn	no	R10
HD 219623	6134	4.14	unkn	no	R10
HD 220117	6351	3.49	unkn	no	R10
HD 222368	6378	4.19	unkn	no	R10
HD 224930	5706	4.81	unkn	no	R10
HD 225239	5522	3.82	unkn	no	R10
Sun	5818	4.38	yes	no	R10
HD 87	5081	2.52	unkn	yes	R11
HD 360	4831	2.74	unkn	yes	R11
HD 448	4749	2.49	unkn	yes	R11
HD 587	4853	3.03	unkn	yes	R11
HD 645	4877	3.07	unkn	yes	R11
HD 1239	5200	2.16	unkn	yes	R11
HD 2114	5143	2.61	unkn	yes	R11
HD 2952	4854	2.58	unkn	yes	R11
HD 3421	5341	1.94	unkn	yes	R11
HD 3546	4854	2.19	unkn	yes	R11
HD 3817	4968	2.46	unkn	yes	R11
HD 3856	4803	2.23	unkn	yes	R11
HD 4188	4943	2.69	unkn	yes	R11
HD 4398	4796	2.53	unkn	yes	R11
HD 4440	4874	2.85	unkn	yes	R11
HD 4627	4537	1.86	unkn	yes	R11
HD 4732	4863	3.21	unkn	yes	R11
HD 5395	4726	2.11	unkn	yes	R11
HD 5608	4895	3.02	unkn	yes	R11
HD 5722	4844	2.38	unkn	yes	R11
HD 6186	4763	2.33	unkn	yes	R11
HD 7087	5000	2.32	unkn	yes	R11
HD 9057	4920	2.54	unkn	yes	R11
HD 9408	4823	2.27	unkn	yes	R11
HD 9774	5112	2.57	unkn	yes	R11
HD 10348	4967	2.57	unkn	yes	R11
HD 10761	4931	2.36	unkn	yes	R11

Table 1. Continued.

Star	T _{eff} [K]	log g [dex]	Exoplanet Host	Giant Star	Equivalent Width Ref.
HD 10975	4841	2.54	unkn	yes	R11
HD 11037	4922	2.39	unkn	yes	R11
HD 11949	4949	2.75	unkn	yes	R11
HD 12139	4711	2.42	unkn	yes	R11
HD 12339	5014	2.43	unkn	yes	R11
HD 12583	4970	2.41	unkn	yes	R11
HD 13468	4798	2.63	unkn	yes	R11
HD 13692	4896	2.52	unkn	yes	R11
HD 13994	5071	2.44	unkn	yes	R11
HD 14129	4843	2.60	unkn	yes	R11
HD 14770	5036	2.49	unkn	yes	R11
HD 15779	4781	2.67	unkn	yes	R11
HD 15920	5084	2.85	unkn	yes	R11
HD 16400	4841	2.40	unkn	yes	R11
HD 16901	5645	1.41	unkn	yes	R11
HD 17656	5034	2.74	unkn	yes	R11
HD 17824	5113	2.88	unkn	yes	R11
HD 18474	4922	2.50	unkn	yes	R11
HD 18953	4952	3.11	unkn	yes	R11
HD 18970	4834	2.36	unkn	yes	R11
HD 19476	4935	2.88	unkn	yes	R11
HD 19525	4799	2.67	unkn	yes	R11
HD 19845	5029	2.96	unkn	yes	R11
HD 20618	5000	3.14	unkn	yes	R11
HD 20791	5047	2.74	unkn	yes	R11
HD 20894	5100	2.70	unkn	yes	R11
HD 21755	5066	2.37	unkn	yes	R11
HD 22409	5044	2.74	unkn	yes	R11
HD 22675	4882	2.42	unkn	yes	R11
HD 22796	5021	2.64	unkn	yes	R11
HD 23526	4803	2.45	unkn	yes	R11
HD 26409	5010	2.66	unkn	yes	R11
HD 27022	5293	2.98	unkn	yes	R11
HD 27348	5031	2.68	unkn	yes	R11
HD 27371	4840	2.59	unkn	yes	R11
HD 27697	4989	2.72	unkn	yes	R11
HD 27971	4796	2.65	unkn	yes	R11
HD 28100	5009	2.71	unkn	yes	R11
HD 28305	4940	2.55	yes	yes	R11
HD 28307	4903	2.53	unkn	yes	R11
HD 29737	4925	2.26	unkn	yes	R11
HD 30557	4942	2.52	unkn	yes	R11
HD 30814	4786	2.65	unkn	yes	R11
HD 32008	5143	3.21	unkn	yes	R11
HD 33833	5032	2.68	unkn	yes	R11
HD 34538	4840	2.87	unkn	yes	R11
HD 34559	4942	2.64	unkn	yes	R11
HD 35369	4944	2.45	unkn	yes	R11
HD 35410	4955	2.64	unkn	yes	R11
HD 36079	5117	2.48	unkn	yes	R11
HD 37160	4711	2.38	unkn	yes	R11
HD 38527	5114	2.87	unkn	yes	R11
HD 38656	4829	2.43	unkn	yes	R11
HD 39004	4924	2.77	unkn	yes	R11
HD 39007	4938	2.84	unkn	yes	R11
HD 39019	5032	2.92	unkn	yes	R11
HD 39364	4581	2.30	unkn	yes	R11
HD 41361	4902	2.16	unkn	yes	R11
HD 41597	4578	1.64	unkn	yes	R11
HD 43023	4968	2.64	unkn	yes	R11

Table 1. Continued.

Star	T _{eff} [K]	log g [dex]	Exoplanet Host	Giant Star	Equivalent Width Ref.
HD 43039	4681	2.23	unkn	yes	R11
HD 45410	5063	3.22	unkn	yes	R11
HD 45415	4735	2.51	unkn	yes	R11
HD 46241	5013	2.69	unkn	yes	R11
HD 46480	4881	2.94	unkn	yes	R11
HD 48432	4884	2.72	unkn	yes	R11
HD 50522	4800	2.62	unkn	yes	R11
HD 51000	5251	2.87	unkn	yes	R11
HD 51814	4816	2.32	unkn	yes	R11
HD 53329	4975	2.47	unkn	yes	R11
HD 54131	4717	2.49	unkn	yes	R11
HD 54810	4629	2.37	unkn	yes	R11
HD 55730	4831	2.36	unkn	yes	R11
HD 57478	4946	2.44	unkn	yes	R11
HD 57727	5055	2.95	unkn	yes	R11
HD 58367	4879	1.79	unkn	yes	R11
HD 60986	4964	2.66	unkn	yes	R11
HD 61363	4701	2.36	unkn	yes	R11
HD 62345	5066	2.44	unkn	yes	R11
HD 62509	4978	2.92	yes	yes	R11
HD 64152	4949	2.85	unkn	yes	R11
HD 65228	5834	1.82	unkn	yes	R11
HD 65345	4949	2.80	unkn	yes	R11
HD 65714	4982	2.42	unkn	yes	R11
HD 67447	5023	2.17	unkn	yes	R11
HD 68077	4911	2.40	unkn	yes	R11
HD 68290	5144	3.04	unkn	yes	R11
HD 68312	5001	2.82	unkn	yes	R11
HD 68375	4947	2.67	unkn	yes	R11
HD 71088	4980	2.83	unkn	yes	R11
HD 71115	5147	2.48	unkn	yes	R11
HD 71369	5282	2.74	unkn	yes	R11
HD 73017	4637	2.47	unkn	yes	R11
HD 73593	4704	2.53	unkn	yes	R11
HD 74395	5289	1.66	unkn	yes	R11
HD 74739	4970	2.15	unkn	yes	R11
HD 74918	5042	2.68	unkn	yes	R11
HD 75506	4821	2.32	unkn	yes	R11
HD 76219	4825	2.09	unkn	yes	R11
HD 76294	4707	2.36	unkn	yes	R11
HD 76813	5002	2.67	unkn	yes	R11
HD 77912	4801	1.84	unkn	yes	R11
HD 78235	5108	3.02	unkn	yes	R11
HD 78668	4916	2.84	unkn	yes	R11
HD 79181	4880	2.55	unkn	yes	R11
HD 79452	4984	2.26	unkn	yes	R11
HD 80499	4997	2.52	unkn	yes	R11
HD 81688	4792	2.17	yes	yes	R11
HD 82087	4821	2.58	unkn	yes	R11
HD 82210	5298	3.36	unkn	yes	R11
HD 82734	4890	2.68	unkn	yes	R11
HD 82741	4840	2.35	unkn	yes	R11
HD 83506	4842	2.31	unkn	yes	R11
HD 83805	5060	2.63	unkn	yes	R11
HD 84441	5374	2.14	unkn	yes	R11
HD 85444	5110	2.53	unkn	yes	R11
HD 91190	4941	2.69	unkn	yes	R11
HD 91612	4920	2.67	unkn	yes	R11
HD 92125	5389	2.12	unkn	yes	R11
HD 93291	5045	2.69	unkn	yes	R11

Table 1. Continued.

Star	T _{eff} [K]	log g [dex]	Exoplanet Host	Giant Star	Equivalent Width Ref.
HD 94402	5103	2.58	unkn	yes	R11
HD 94497	4838	2.85	unkn	yes	R11
HD 95808	4903	2.75	unkn	yes	R11
HD 98839	4847	2.23	unkn	yes	R11
HD 99055	5086	2.61	unkn	yes	R11
HD 99283	4810	2.52	unkn	yes	R11
HD 99648	4977	2.49	unkn	yes	R11
HD 100615	4866	2.45	unkn	yes	R11
HD 100696	4743	2.32	unkn	yes	R11
HD 100920	4810	2.66	unkn	yes	R11
HD 101484	4857	2.74	unkn	yes	R11
HD 102070	5000	2.57	unkn	yes	R11
HD 103462	4921	2.26	unkn	yes	R11
HD 103484	5085	3.25	unkn	yes	R11
HD 104979	4903	2.58	unkn	yes	R11
HD 104985	4713	2.40	yes	yes	R11
HD 106057	4966	2.73	unkn	yes	R11
HD 106714	4989	2.49	unkn	yes	R11
HD 107383	4848	2.49	bd	yes	R11
HD 107950	5095	2.68	unkn	yes	R11
HD 108225	4870	2.71	unkn	yes	R11
HD 109272	5052	3.30	unkn	yes	R11
HD 109317	4830	2.52	unkn	yes	R11
HD 109379	5134	2.58	unkn	yes	R11
HD 110646	5125	3.09	unkn	yes	R11
HD 111028	4810	3.15	unkn	yes	R11
HD 113095	4953	2.74	unkn	yes	R11
HD 113226	5108	2.72	unkn	yes	R11
HD 114256	4989	2.50	unkn	yes	R11
HD 115202	4830	3.04	unkn	yes	R11
HD 115659	5006	2.47	unkn	yes	R11
HD 116292	4824	2.42	unkn	yes	R11
HD 116957	4938	2.78	unkn	yes	R11
HD 117566	5397	3.24	unkn	yes	R11
HD 117818	4736	2.21	unkn	yes	R11
HD 118219	4918	2.24	unkn	yes	R11
HD 119126	4777	2.21	unkn	yes	R11
HD 119605	5455	1.92	unkn	yes	R11
HD 120048	5145	2.81	unkn	yes	R11
HD 120084	4841	2.73	unkn	yes	R11
HD 120420	4775	2.67	unkn	yes	R11
HD 120787	4894	2.26	unkn	yes	R11
HD 125454	4916	2.53	unkn	yes	R11
HD 126218	5070	2.51	unkn	yes	R11
HD 127243	4835	2.19	unkn	yes	R11
HD 129312	5075	2.51	unkn	yes	R11
HD 129336	4854	2.64	unkn	yes	R11
HD 129944	4805	2.52	unkn	yes	R11
HD 129972	4915	2.65	unkn	yes	R11
HD 130952	4754	2.26	unkn	yes	R11
HD 131530	5032	2.83	unkn	yes	R11
HD 132146	5010	2.30	unkn	yes	R11
HD 133002	5519	3.40	unkn	yes	R11
HD 133208	4864	2.33	unkn	yes	R11
HD 133392	4911	2.51	unkn	yes	R11
HD 134190	4762	2.44	unkn	yes	R11
HD 136512	4797	2.41	unkn	yes	R11
HD 136956	5105	2.72	unkn	yes	R11
HD 138716	4823	3.16	unkn	yes	R11
HD 138852	4857	2.45	unkn	yes	R11

Table 1. Continued.

Star	T _{eff} [K]	log g [dex]	Exoplanet Host	Giant Star	Equivalent Width Ref.
HD 138905	4760	2.66	unkn	yes	R11
HD 139641	4868	2.81	unkn	yes	R11
HD 141680	4796	2.38	unkn	yes	R11
HD 142091	4824	3.19	yes	yes	R11
HD 142198	4855	2.19	unkn	yes	R11
HD 142531	4899	2.83	unkn	yes	R11
HD 143553	4742	2.73	unkn	yes	R11
HD 144608	5221	2.58	unkn	yes	R11
HD 145001	5211	2.79	unkn	yes	R11
HD 146791	4955	2.73	unkn	yes	R11
HD 147677	5063	2.93	unkn	yes	R11
HD 147700	4900	2.51	unkn	yes	R11
HD 148387	5008	2.69	unkn	yes	R11
HD 148604	5096	2.96	unkn	yes	R11
HD 148786	5118	2.63	unkn	yes	R11
HD 150030	4943	2.17	unkn	yes	R11
HD 150997	4989	2.76	unkn	yes	R11
HD 152815	4987	2.47	unkn	yes	R11
HD 154084	4771	2.51	unkn	yes	R11
HD 154779	5132	2.79	unkn	yes	R11
HD 156874	4952	2.90	unkn	yes	R11
HD 156891	4894	2.98	unkn	yes	R11
HD 157527	5078	3.00	unkn	yes	R11
HD 158974	4921	2.35	unkn	yes	R11
HD 159181	5180	1.62	unkn	yes	R11
HD 159353	4902	2.67	unkn	yes	R11
HD 160781	4686	2.08	unkn	yes	R11
HD 161178	4690	2.17	unkn	yes	R11
HD 162076	4918	3.00	unkn	yes	R11
HD 163532	4542	2.28	unkn	yes	R11
HD 163917	4908	2.57	unkn	yes	R11
HD 165760	4964	2.59	unkn	yes	R11
HD 167042	4864	3.39	yes	yes	R11
HD 167768	4851	2.01	unkn	yes	R11
HD 168656	4996	2.75	unkn	yes	R11
HD 168723	4982	3.06	unkn	yes	R11
HD 170474	4894	2.82	unkn	yes	R11
HD 171391	5122	2.75	unkn	yes	R11
HD 174980	5024	2.73	unkn	yes	R11
HD 176598	4955	2.98	unkn	yes	R11
HD 176707	4735	2.27	unkn	yes	R11
HD 177241	4907	2.64	unkn	yes	R11
HD 177249	5263	2.53	unkn	yes	R11
HD 180540	5042	2.26	unkn	yes	R11
HD 180711	4978	2.69	unkn	yes	R11
HD 181276	5036	2.83	unkn	yes	R11
HD 182694	5074	2.60	unkn	yes	R11
HD 182762	4795	2.58	unkn	yes	R11
HD 183491	4974	2.67	unkn	yes	R11
HD 184010	4995	3.24	unkn	yes	R11
HD 185018	5492	1.78	unkn	yes	R11
HD 185194	4934	2.32	unkn	yes	R11
HD 185351	4957	3.14	unkn	yes	R11
HD 185467	4966	2.66	unkn	yes	R11
HD 185758	5534	2.43	unkn	yes	R11
HD 185958	4760	2.14	unkn	yes	R11
HD 186675	4887	2.53	unkn	yes	R11
HD 187739	4690	2.76	unkn	yes	R11
HD 188310	4920	2.70	yes	yes	R11
HD 188650	5473	1.87	unkn	yes	R11

Table 1. Continued.

Star	T _{eff} [K]	log g [dex]	Exoplanet Host	Giant Star	Equivalent Width Ref.
HD 188947	4941	2.58	unkn	yes	R11
HD 189127	4737	2.17	unkn	yes	R11
HD 192787	4932	2.83	unkn	yes	R11
HD 192879	4902	2.68	unkn	yes	R11
HD 192944	5011	2.49	unkn	yes	R11
HD 192947	5119	2.94	unkn	yes	R11
HD 194013	4966	2.54	unkn	yes	R11
HD 194577	5060	2.71	unkn	yes	R11
HD 196857	4830	2.47	unkn	yes	R11
HD 199665	4848	2.74	yes	yes	R11
HD 200039	4896	2.65	unkn	yes	R11
HD 201381	4902	2.84	unkn	yes	R11
HD 203222	5039	2.86	unkn	yes	R11
HD 203387	5285	3.03	unkn	yes	R11
HD 204381	5079	2.80	unkn	yes	R11
HD 204771	5107	3.00	unkn	yes	R11
HD 205072	4932	2.66	unkn	yes	R11
HD 205435	5119	3.12	unkn	yes	R11
HD 206356	4896	2.92	unkn	yes	R11
HD 206453	4976	2.53	unkn	yes	R11
HD 209396	5021	2.78	unkn	yes	R11
HD 210354	4720	2.46	unkn	yes	R11
HD 210434	4854	2.98	unkn	yes	R11
HD 210702	4964	3.12	yes	yes	R11
HD 210807	5122	2.57	unkn	yes	R11
HD 211391	4952	2.69	unkn	yes	R11
HD 211434	5069	2.74	unkn	yes	R11
HD 211554	5071	2.53	unkn	yes	R11
HD 212271	5092	2.93	unkn	yes	R11
HD 212320	5156	2.70	unkn	yes	R11
HD 212430	4933	2.51	unkn	yes	R11
HD 212496	4779	2.52	unkn	yes	R11
HD 213789	4997	2.74	unkn	yes	R11
HD 213930	5084	2.81	unkn	yes	R11
HD 213986	4964	2.92	unkn	yes	R11
HD 214567	4927	2.60	unkn	yes	R11
HD 214878	4941	3.00	unkn	yes	R11
HD 215030	4878	2.51	unkn	yes	R11
HD 215373	4865	2.77	unkn	yes	R11
HD 215721	4736	2.25	unkn	yes	R11
HD 215943	4815	2.73	unkn	yes	R11
HD 216131	4987	2.65	unkn	yes	R11
HD 217264	4879	2.95	unkn	yes	R11
HD 217703	4795	2.99	unkn	yes	R11
HD 218527	4789	2.62	unkn	yes	R11
HD 219139	4868	2.43	unkn	yes	R11
HD 219615	4746	2.34	unkn	yes	R11
HD 219945	4897	2.51	unkn	yes	R11
HD 221345	4855	2.58	unkn	yes	R11
HD 222093	4936	2.53	unkn	yes	R11
HD 222387	5056	2.69	unkn	yes	R11
HD 222574	5476	1.92	unkn	yes	R11
HD 223252	4921	2.65	unkn	yes	R11
HD 224533	5039	2.82	unkn	yes	R11

References: R1: González (1998), R2: González et al. (1999), R3: González & Laws (2000), R4: González et al. (2001), R5: Laws & González (2001), R6: Sadakane et al. (2005), R7: Santos et al. (2000), R8: Laws et al. (2003), R9: Zhao et al. (2002), R10: Takeda et al. (2005), R11: Takeda et al. (2008).

Table 2. ξ , [Fe/H], τ and Σ derived for the sample stars.

Star	ξ	[FeI/H]	σ_{FeI}	n ₁	[FeII/H]	σ_{FeII}	n ₂	τ_{FeI}	τ_{FeII}	Σ
rho crb	0,80	-0,24	0,06	13	-0,20	0,14	2	0,40	0,42	-0,015
47 Uma = HR 4277	1,00	-0,11	0,11	9	-0,22	0,01	2	0,16	0,30	0,018
70 Vir = HR 5072	0,60	-0,01	0,10	9	-0,15	0,04	2	0,20	0,44	0,137
HD 114762	1,30	-0,91	0,00	1	-0,77	0,00	2	0,12	0,42	
14 her = GJ 614	0,30	0,48	0,15	8	7,81	0,00	1	0,13	0,57	-0,114
HD 75289	1,30	0,22	0,12	23	0,20	0,13	3	0,27	0,09	0,025
nu and	1,30	0,03	0,12	11	0,09	0,00	1	0,40	0,46	0,040
tau boo	1,30	0,22	0,12	11	0,28	0,00	1	0,30	0,28	0,019
rho cnc	0,90	0,22	0,12	17	0,25	0,25	4	0,29	0,53	0,074
HD 75332	1,00	0,17	0,09	12	-0,66	0,00	1	0,32	0,38	0,024
HD 192263	0,80	-0,06	0,05	13	-0,11	0,00	1	0,29	0,59	0,020
HD 209458	1,40	-0,08	0,13	16	-0,06	0,22	3	0,43	0,33	0,126
51 Peg = HR 8729	1,40	0,11	0,13	14	-0,64	0,00	1	0,33	0,52	0,093
HD 222582	1,10	-0,05	0,13	13	-0,82	0,00	1	0,42	0,63	0,112
HR 810	2,50	-0,01	0,17	8	0,00	0,00	1	0,42	0,40	-0,341
16 cyg A = HR 750	0,90	0,03	0,13	22	0,10	0,17	3	0,38	0,45	0,076
16 cyg B = HR 750	0,70	0,02	0,12	22	0,09	0,14	3	0,35	0,45	0,035
HD 47536	1,50	-0,62	0,10	31	-0,57	0,11	3	1,20	1,55	-0,029
HD 59686	1,50	-0,04	0,09	26	-0,01	0,19	3	0,82	1,32	-0,017
HD 137759	1,40	-0,01	0,11	26	0,05	0,19	3	0,80	1,30	-0,029
HD 219449	1,50	-0,11	0,08	29	-0,07	0,14	3	0,82	1,26	-0,028
HD 1237	0,90	0,14	0,11	18	0,13	0,21	3	0,06	0,25	-0,135
HD 13445	0,00	-0,22	0,08	19	-0,11	0,23	3	0,18	0,42	0,037
HD 83443	0,00	0,42	0,13	19	0,45	0,20	3	-0,05	0,19	-0,149
HD 4203	1,10	0,34	0,14	26	0,39	0,23	3	0,30	0,43	-0,003
HD 4208	0,60	-0,29	0,11	25	-0,14	0,20	3	0,49	0,51	0,037
HD 6434	0,20	-0,59	0,13	26	-0,44	0,17	3	0,63	0,58	-0,004
HD 8574	0,90	-0,02	0,09	27	-0,02	0,14	4	0,50	0,39	-0,004
HD 28185	0,40	0,23	0,08	26	0,30	0,17	3	0,20	0,31	-0,048
HD 37124	0,00	-0,40	0,11	25	-0,28	0,18	3	0,50	0,52	0,027
HD 46375	0,00	0,25	0,10	25	0,34	0,19	3	0,20	0,46	0,023
HD 68988	1,10	0,27	0,12	26	0,33	0,20	3	0,28	0,28	0,036
HD 106252	0,80	-0,08	0,11	27	-0,05	0,19	4	0,43	0,40	0,039
HD 114783	0,00	0,13	0,09	26	0,08	0,08	2	0,23	0,44	0,039
HD 136118	1,40	-0,08	0,12	26	-0,05	0,11	3	0,48	0,34	0,085
HD 141937	0,80	0,09	0,11	27	0,16	0,15	3	0,34	0,34	0,006
HD 168746	0,70	-0,09	0,11	27	0,00	0,20	3	0,41	0,47	0,036
HD 202206	0,90	0,28	0,12	27	0,35	0,18	3	0,23	0,32	0,002
HD 27442	0,80	0,37	0,18	24	0,51	0,11	2	0,52	0,95	-0,070
HD 108147	1,20	0,10	0,17	25	0,21	0,02	3	0,31	0,29	-0,028
HD 121504	0,80	0,09	0,16	23	0,18	0,11	3	0,39	0,46	0,020
HD 160691	1,00	0,21	0,12	21	0,16	0,00	1	0,31	0,41	0,062
HD 213240	0,90	0,19	0,13	24	0,26	0,04	3	0,29	0,35	-0,002
HD 12661	1,30	0,26	0,16	42	0,19	0,13	4	0,00	0,35	0,370
HD 19994	1,20	0,13	0,14	39	0,12	0,11	4	0,32	0,37	0,016
HD 29587	0,40	-0,54	0,14	39	-0,44	0,09	4	0,39	0,60	0,020
HD 92788	0,90	0,20	0,20	37	0,36	0,21	4	0,04	0,28	0,137
HD 98230	0,50	-0,22	0,12	39	-0,10	0,23	3	0,27	0,45	-0,001
HD 120136	1,60	0,26	0,18	28	0,20	0,12	4	0,21	0,20	0,129
HD 187123	0,70	0,13	0,14	30	0,14	0,12	3	0,16	0,42	0,090
HD 190228	0,50	-0,16	0,14	38	-0,08	0,13	4	0,39	0,79	0,047
HD 123	1,20	-0,01	0,18	103	-0,01	0,27	5	0,25	0,21	-0,047
HD 400	1,20	-0,28	0,12	95	-0,34	0,06	4	0,62	0,47	0,096
HD 693	1,10	-0,37	0,13	95	-0,39	0,09	5	0,62	0,52	0,072
HD 4307	1,00	-0,28	0,15	102	-0,28	0,04	4	0,77	0,72	0,003
HD 4614	0,80	-0,23	0,13	112	-0,22	0,11	6	0,46	0,47	0,034
HD 4628	0,20	-0,24	0,13	118	-0,29	0,09	4	0,41	0,55	0,011
HD 4813	1,00	-0,08	0,11	107	-0,07	0,09	6	0,40	0,33	0,043
HD 5015	1,20	0,08	0,12	103	0,04	0,13	3	0,51	0,47	0,057
HD 6582	0,20	-0,79	0,12	109	-0,75	0,08	4	0,54	0,57	0,022

Table 2. Continued.

Star	ξ	[FeI/H]	σ_{FeI}	n ₁	[FeII/H]	σ_{FeII}	n ₂	τ_{FeI}	τ_{FeII}	Σ
HD 6920	1,60	-0,07	0,13	77	-0,08	0,10	3	0,67	0,66	0,121
HD 7439	1,10	-0,35	0,14	82	-0,30	0,16	5	0,61	0,39	0,033
HD 7476	1,20	-0,29	0,14	74	-0,23	0,15	4	0,68	0,52	-0,027
HD 9562	1,30	0,18	0,12	107	0,13	0,09	4	0,46	0,47	0,052
HD 9826	1,40	0,02	0,11	92	-0,01	0,07	4	0,56	0,47	0,063
HD 10307	1,00	0,01	0,12	118	0,00	0,10	6	0,42	0,45	0,027
HD 10476	0,50	-0,04	0,12	114	-0,07	0,14	5	0,36	0,52	0,038
HD 10697	1,10	0,07	0,12	114	-0,01	0,14	4	0,56	0,57	0,058
HD 10700	0,50	-0,44	0,11	126	-0,51	0,02	3	0,42	0,46	0,011
HD 10780	0,80	0,03	0,12	114	0,02	0,17	5	0,30	0,45	0,034
HD 13555	1,40	-0,27	0,14	83	-0,26	0,05	4	0,54	0,52	0,079
HD 14214	1,20	0,10	0,12	111	0,08	0,09	6	0,49	0,50	0,044
HD 15335	1,20	-0,24	0,12	114	-0,26	0,10	5	0,74	0,60	0,070
HD 15798	1,30	-0,30	0,13	77	-0,31	0,09	3	0,72	0,64	0,083
HD 16141	1,10	0,07	0,12	111	0,04	0,12	7	0,55	0,57	0,072
HD 16673	1,20	0,00	0,12	94	-0,08	0,03	4	0,38	0,24	0,060
HD 16895	1,40	-0,01	0,12	91	-0,09	0,09	3	0,42	0,40	0,072
HD 17925	0,90	0,11	0,12	92	-0,01	0,22	3	0,33	0,40	-0,038
HD 18803	0,80	0,09	0,13	116	0,01	0,12	4	0,33	0,38	0,018
HD 20630	1,00	0,06	0,12	111	0,03	0,15	5	0,33	0,39	0,043
HD 21019	0,80	-0,47	0,11	116	-0,42	0,16	6	0,82	0,83	0,005
HD 22049	0,80	-0,05	0,12	121	0,00	0,27	4	0,32	0,47	0,021
HD 22484	1,20	-0,10	0,10	109	-0,12	0,07	3	0,59	0,45	0,018
HD 30562	1,20	0,18	0,12	107	0,09	0,10	4	0,48	0,46	0,055
HD 30743	1,20	-0,52	0,13	63	-0,56	0,07	4	0,67	0,54	0,107
HD 32923	1,00	-0,24	0,12	118	-0,24	0,09	6	0,68	0,65	0,074
HD 33636	0,90	-0,11	0,12	112	-0,14	0,08	5	0,40	0,38	0,060
HD 34411	1,00	0,06	0,11	105	0,01	0,08	6	0,47	0,49	0,005
HD 35296	1,30	0,03	0,12	50	-0,04	0,00	1	0,41	0,46	0,000
HD 38529	1,30	0,25	0,13	106	0,20	0,07	3	0,56	0,66	0,029
HD 39587	1,10	-0,05	0,13	88	-0,11	0,10	4	0,37	0,26	0,070
HD 43042	1,40	0,03	0,13	100	0,03	0,01	2	0,40	0,38	0,081
HD 43318	1,30	-0,22	0,12	101	-0,24	0,05	5	0,69	0,61	0,037
HD 49933	1,00	-0,49	0,13	55	-0,48	0,16	4	0,54	0,39	-0,017
HD 50554	1,10	-0,08	0,12	118	-0,12	0,09	6	0,49	0,43	0,062
HD 52265	1,30	0,09	0,12	113	0,09	0,14	5	0,50	0,48	0,046
HD 52711	1,00	-0,14	0,11	108	-0,19	0,08	5	0,50	0,42	0,073
HD 55575	0,90	-0,35	0,13	103	-0,38	0,04	6	0,57	0,53	0,066
HD 59984	0,70	-0,68	0,12	83	-0,66	0,08	5	0,72	0,61	-0,022
HD 61421	1,50	-0,08	0,11	104	-0,07	0,06	4	0,51	0,44	0,067
HD 67228	1,30	0,06	0,12	111	0,06	0,12	6	0,62	0,67	0,085
HD 67767	1,00	-0,10	0,12	115	-0,07	0,18	5	0,73	0,87	0,062
HD 69830	0,70	-0,05	0,12	110	-0,07	0,17	5	0,34	0,49	0,045
HD 69897	1,00	-0,34	0,11	95	-0,32	0,07	5	0,61	0,43	0,022
HD 70110	1,20	0,08	0,12	108	0,04	0,10	4	0,57	0,61	0,037
HD 75732	0,40	0,39	0,13	103	0,28	0,10	3	0,17	0,27	-0,068
HD 76151	0,90	0,07	0,12	116	0,02	0,07	7	0,36	0,41	0,041
HD 76932	0,20	-0,90	0,11	83	-0,83	0,13	5	0,70	0,64	-0,031
HD 79028	1,20	-0,04	0,12	113	-0,05	0,11	6	0,60	0,50	0,079
HD 81809	0,90	-0,34	0,11	107	-0,36	0,07	6	0,66	0,65	0,055
HD 82328	1,60	-0,32	0,12	90	-0,33	0,08	4	0,77	0,65	0,132
HD 82885	1,00	0,26	0,12	107	0,22	0,12	5	0,29	0,40	0,001
HD 82943	1,00	0,23	0,12	114	0,19	0,07	4	0,32	0,41	0,008
HD 84737	1,30	0,06	0,12	112	0,05	0,11	6	0,56	0,59	0,096
HD 86728	1,00	0,21	0,12	110	0,12	0,12	4	0,32	0,32	0,031
HD 87141	1,90	0,00	0,12	41	-0,21	0,02	2	0,53	0,48	0,024
HD 88737	1,70	0,13	0,12	78	0,12	0,16	4	0,60	0,61	0,108
HD 88986	1,00	0,03	0,11	118	-0,02	0,08	7	0,50	0,51	0,024
HD 89125	1,00	-0,41	0,11	91	-0,41	0,06	4	0,61	0,48	0,056
HD 89744	1,60	0,09	0,12	86	0,06	0,08	5	0,58	0,53	0,051
HD 91752	1,40	-0,12	0,13	45	-0,15	0,02	2	0,31	0,23	0,031

Table 2. Continued.

Star	ξ	[FeI/H]	σ_{FeI}	n ₁	[FeII/H]	σ_{FeII}	n ₂	τ_{FeI}	τ_{FeII}	Σ
HD 91889	0,90	-0,24	0,10	109	-0,24	0,12	6	0,60	0,49	0,022
HD 95128	1,10	-0,04	0,13	125	-0,02	0,13	7	0,48	0,46	0,056
HD 95241	1,20	-0,31	0,12	106	-0,32	0,02	3	0,80	0,65	0,043
HD 98991	1,60	-0,19	0,14	34	-0,15	0,00	1	0,75	0,66	0,096
HD 99491	1,20	0,16	0,10	61	0,22	0,19	5	0,37	0,53	0,061
HD 99747	0,90	-0,36	0,13	41	-0,30	0,19	3	0,24	0,01	-0,043
HD 101501	0,90	-0,08	0,12	118	-0,08	0,16	3	0,37	0,45	0,045
HD 102634	1,40	0,14	0,12	103	0,10	0,08	4	0,44	0,33	0,027
HD 102870	1,30	0,07	0,12	121	0,08	0,09	6	0,53	0,50	0,045
HD 104304	0,90	0,18	0,13	115	0,15	0,16	6	0,34	0,46	0,038
HD 107213	1,60	0,20	0,13	88	0,15	0,07	2	0,50	0,49	0,013
HD 109358	0,90	-0,25	0,11	118	-0,23	0,12	7	0,50	0,48	0,025
HD 110897	0,70	-0,53	0,12	96	-0,53	0,06	4	0,57	0,52	0,022
HD 111395	0,90	0,05	0,12	120	0,04	0,16	7	0,34	0,44	0,030
HD 114642	1,40	-0,16	0,12	55	-0,14	0,11	3	0,59	0,39	0,039
HD 114710	1,00	0,07	0,12	109	0,04	0,15	5	0,36	0,30	0,032
HD 114946	0,90	-0,33	0,13	116	-0,27	0,17	5	0,95	1,10	0,053
HD 115383	1,30	0,13	0,13	103	0,19	0,15	3	0,43	0,54	0,077
HD 115617	0,70	0,06	0,12	110	0,00	0,13	3	0,27	0,33	0,005
HD 117176	1,00	-0,15	0,11	129	-0,14	0,14	6	0,69	0,73	0,040
HD 121370	1,70	0,27	0,15	48	0,26	0,00	1	0,43	0,35	0,058
HD 122742	0,80	-0,04	0,13	116	0,06	0,26	4	0,45	0,58	0,012
HD 124570	1,50	0,00	0,13	100	-0,02	0,09	4	0,64	0,65	0,047
HD 124850	1,50	-0,02	0,10	42	-0,38	0,00	1	0,47	0,43	-0,013
HD 125184	1,10	0,20	0,13	111	0,21	0,00	2	0,48	0,68	0,013
HD 127334	1,00	0,16	0,12	115	0,10	0,08	4	0,37	0,47	0,040
HD 128167	1,30	-0,34	0,10	48	-0,29	0,07	3	0,24	0,07	0,001
HD 131156	1,00	-0,17	0,14	108	-0,24	0,08	3	0,38	0,39	0,051
HD 131511	0,90	0,02	0,12	105	-0,02	0,16	2	0,34	0,40	0,043
HD 134987	1,00	0,22	0,13	119	0,13	0,13	6	0,32	0,36	0,041
HD 136064	1,30	-0,01	0,12	96	-0,07	0,07	3	0,56	0,44	0,049
HD 137052	1,40	0,04	0,13	54	0,00	0,12	4	0,38	0,27	0,004
HD 137108	1,00	-0,09	0,13	108	-0,04	0,18	6	0,54	0,52	0,027
HD 137510	1,40	0,35	0,13	91	0,40	0,06	3	0,33	0,43	0,016
HD 141004	1,10	-0,06	0,12	106	-0,06	0,14	7	0,56	0,54	0,085
HD 142373	0,80	-0,52	0,11	103	-0,45	0,13	7	0,78	0,73	0,026
HD 142860	1,00	-0,14	0,11	58	-0,17	0,10	4	0,53	0,38	0,013
HD 143761	0,90	-0,25	0,11	127	-0,26	0,08	6	0,55	0,51	0,008
HD 144585	1,10	0,23	0,12	110	0,22	0,01	2	0,42	0,58	0,029
HD 145675	0,70	0,36	0,13	104	0,33	0,16	6	0,24	0,41	0,015
HD 149661	0,60	0,01	0,12	112	-0,07	0,11	2	0,31	0,39	-0,008
HD 150706	1,20	-0,09	0,16	84	-0,14	0,21	5	0,40	0,36	0,080
HD 151769	1,60	-0,11	0,13	62	-0,13	0,12	4	0,83	0,66	0,067
HD 153597	1,20	-0,12	0,12	63	-0,12	0,14	5	0,37	0,25	0,030
HD 156826	0,90	-0,24	0,12	116	-0,25	0,22	5	0,78	0,94	0,011
HD 157214	0,80	-0,40	0,12	112	-0,38	0,20	5	0,60	0,61	0,040
HD 161797	1,20	0,21	0,13	117	0,14	0,17	5	0,48	0,58	0,046
HD 163989	1,30	-0,06	0,12	98	-0,01	0,10	6	0,59	0,52	-0,041
HD 165341	0,80	-0,01	0,12	112	-0,03	0,17	2	0,35	0,41	0,040
HD 165908	0,80	-0,50	0,13	84	-0,47	0,01	3	0,52	0,40	0,027
HD 168009	0,90	0,00	0,12	116	-0,02	0,10	6	0,40	0,47	0,017
HD 168151	1,40	-0,33	0,12	63	-0,38	0,04	4	0,48	0,29	0,087
HD 168443	1,00	0,03	0,13	123	-0,07	0,07	4	0,49	0,56	0,054
HD 169830	1,30	0,10	0,11	114	0,13	0,01	2	0,48	0,48	0,052
HD 173667	1,50	-0,03	0,12	37	-0,29	0,00	1	0,36	0,29	-0,004
HD 178428	1,00	0,10	0,13	113	0,07	0,17	5	0,44	0,51	0,036
HD 179949	1,20	0,15	0,12	90	0,14	0,02	3	0,30	0,30	0,029
HD 181096	1,20	-0,25	0,13	75	-0,18	0,12	4	0,61	0,49	0,030
HD 181655	0,80	0,10	0,12	119	-0,05	0,07	4	0,29	0,25	0,046
HD 182488	0,60	0,16	0,12	115	0,10	0,12	4	0,25	0,39	0,003
HD 182572	1,00	0,28	0,13	103	0,21	0,13	6	0,41	0,48	0,022

Table 2. Continued.

Star	ξ	[FeI/H]	σ_{FeI}	n ₁	[FeII/H]	σ_{FeII}	n ₂	τ_{FeI}	τ_{FeII}	Σ
HD 185144	0,60	-0,18	0,13	115	-0,16	0,24	6	0,38	0,55	0,015
HD 186408	1,10	0,01	0,12	115	-0,02	0,10	7	0,47	0,49	0,072
HD 186427	0,80	0,09	0,11	119	0,04	0,11	7	0,35	0,40	0,033
HD 187013	1,30	-0,04	0,11	64	-0,04	0,03	2	0,41	0,44	0,030
HD 187691	1,40	0,04	0,12	111	0,09	0,12	5	0,56	0,58	0,092
HD 190406	1,10	0,00	0,13	109	0,02	0,13	6	0,41	0,43	0,071
HD 193664	0,80	-0,08	0,13	109	-0,14	0,07	5	0,38	0,38	0,034
HD 195019	1,00	0,02	0,13	119	-0,02	0,13	5	0,51	0,45	0,030
HD 196755	1,10	0,07	0,12	120	0,01	0,08	3	0,62	0,60	0,009
HD 197076	0,80	-0,10	0,11	107	-0,14	0,10	5	0,44	0,41	0,025
HD 199960	1,20	0,19	0,13	113	0,18	0,16	4	0,40	0,49	0,067
HD 200790	1,30	-0,05	0,13	92	-0,11	0,05	3	0,60	0,57	0,062
HD 207978	1,00	-0,51	0,12	63	-0,48	0,08	3	0,54	0,38	-0,071
HD 210277	0,80	0,18	0,13	115	0,14	0,18	5	0,30	0,44	0,017
HD 210855	1,60	0,00	0,12	62	-0,19	0,00	1	0,73	0,55	0,024
HD 215648	1,00	-0,22	0,11	73	-0,24	0,03	3	0,61	0,39	0,023
HD 216385	1,10	-0,22	0,13	98	-0,27	0,09	3	0,66	0,60	0,047
HD 217014	1,10	0,12	0,12	125	0,11	0,14	6	0,42	0,48	0,068
HD 217107	1,10	0,21	0,14	116	0,21	0,21	5	0,39	0,51	0,072
HD 218470	1,20	-0,13	0,13	51	-0,18	0,03	3	0,54	0,50	0,123
HD 219623	1,20	0,01	0,12	105	0,00	0,09	4	0,50	0,41	0,067
HD 220117	1,80	-0,07	0,12	42	-0,17	0,11	2	0,68	0,56	-0,020
HD 222368	1,10	-0,08	0,13	92	-0,10	0,20	5	0,50	0,42	0,027
HD 224930	0,00	-0,57	0,13	105	-0,67	0,07	3	0,36	0,37	0,051
HD 225239	0,80	-0,41	0,12	107	-0,40	0,11	5	0,73	0,72	-0,024
Sun	0,90	-0,04	0,12	122	-0,07	0,11	7	0,40	0,45	0,034
HD 87	1,20	-0,05	0,13	74	-0,10	0,08	3	1,10	1,19	0,032
HD 360	1,20	-0,06	0,14	74	-0,07	0,15	3	1,08	1,26	0,018
HD 448	1,20	0,06	0,15	62	0,03	0,22	2	1,10	1,16	0,015
HD 587	1,00	-0,08	0,13	76	-0,18	0,07	2	0,91	1,00	0,067
HD 645	1,00	0,10	0,14	72	0,07	0,20	2	0,86	1,07	0,050
HD 1239	1,40	-0,21	0,13	69	-0,13	0,05	2	1,35	1,52	0,019
HD 2114	1,50	-0,03	0,13	74	-0,01	0,00	2	1,16	1,33	0,050
HD 2952	1,20	0,01	0,13	73	-0,04	0,11	3	1,05	1,24	0,018
HD 3421	1,80	-0,18	0,13	58	-0,17	0,11	2	1,54	1,58	-0,015
HD 3546	1,10	-0,62	0,12	75	-0,50	0,04	3	1,46	1,52	-0,030
HD 3817	1,20	-0,08	0,13	69	-0,11	0,08	3	1,13	1,23	0,025
HD 3856	1,20	-0,11	0,14	67	-0,10	0,15	3	1,23	1,42	0,048
HD 4188	1,20	0,02	0,14	65	0,00	0,13	3	1,06	1,26	0,050
HD 4398	1,20	-0,15	0,13	75	-0,19	0,07	3	1,15	1,29	0,023
HD 4440	1,00	-0,08	0,14	76	-0,12	0,11	3	0,98	1,18	0,042
HD 4627	1,30	-0,18	0,13	64	-0,19	0,15	3	1,38	1,58	0,065
HD 4732	1,00	0,02	0,15	77	0,06	0,23	3	0,81	1,03	0,050
HD 5395	1,20	-0,39	0,13	75	-0,34	0,10	3	1,39	1,50	0,034
HD 5608	0,90	0,09	0,15	70	-0,03	0,10	2	0,85	0,99	0,052
HD 5722	1,20	-0,19	0,15	70	-0,19	0,15	2	1,18	1,31	0,027
HD 6186	1,10	-0,24	0,13	72	-0,22	0,07	3	1,27	1,40	0,001
HD 7087	1,40	-0,01	0,13	72	-0,05	0,13	3	1,17	1,31	0,046
HD 9057	1,30	0,03	0,14	69	0,01	0,15	3	1,11	1,27	0,059
HD 9408	1,20	-0,28	0,13	70	-0,25	0,11	3	1,32	1,48	0,038
HD 9774	1,40	0,06	0,14	66	0,02	0,00	1	1,13	1,26	-0,009
HD 10348	1,50	0,02	0,15	70	0,04	0,22	3	1,12	1,24	0,041
HD 10761	1,30	-0,03	0,13	69	-0,04	0,10	3	1,17	1,28	0,043
HD 10975	1,20	-0,14	0,13	76	-0,13	0,12	3	1,18	1,33	0,035
HD 11037	1,20	-0,12	0,13	70	-0,14	0,13	3	1,16	1,33	0,074
HD 11949	1,00	-0,06	0,13	71	-0,05	0,15	3	1,00	1,19	0,033
HD 12139	1,20	-0,06	0,13	74	-0,08	0,15	3	1,13	1,30	-0,008
HD 12339	1,40	-0,01	0,12	71	0,06	0,06	2	1,16	1,39	0,043
HD 12583	1,30	0,04	0,13	70	0,06	0,16	3	1,11	1,22	0,013
HD 13468	1,10	-0,10	0,13	76	-0,15	0,05	3	1,12	1,28	-0,008
HD 13692	1,20	-0,10	0,13	75	-0,07	0,17	3	1,13	1,29	0,030

Table 2. Continued.

Star	ξ	[FeI/H]	σ_{FeI}	n ₁	[FeII/H]	σ_{FeII}	n ₂	τ_{FeI}	τ_{FeII}	Σ
HD 13994	1,50	-0,04	0,13	44	-0,12	0,18	2	1,18	1,13	0,019
HD 14129	1,30	-0,01	0,13	67	-0,04	0,17	3	1,09	1,23	0,071
HD 14770	1,40	0,02	0,15	67	0,00	0,18	2	1,13	1,24	0,056
HD 15779	1,20	-0,01	0,14	71	-0,02	0,16	3	1,06	1,25	0,080
HD 15920	1,10	-0,01	0,14	69	-0,07	0,08	2	1,00	1,12	-0,002
HD 16400	1,20	-0,02	0,14	68	-0,05	0,15	3	1,17	1,37	0,043
HD 16901	2,30	0,00	0,15	37	5,36	0,00	1	1,78	1,82	0,030
HD 17656	1,20	-0,02	0,14	70	0,01	0,14	3	1,04	1,13	0,020
HD 17824	1,00	0,00	0,13	72	-0,03	0,07	3	0,96	1,11	-0,020
HD 18474	1,20	-0,19	0,13	74	-0,20	0,11	3	1,25	1,30	-0,003
HD 18953	1,10	0,16	0,14	75	0,14	0,20	2	0,86	1,03	0,043
HD 18970	1,10	-0,01	0,14	70	0,01	0,16	3	1,12	1,32	-0,011
HD 19476	1,20	0,12	0,15	70	0,11	0,18	3	0,93	1,12	0,078
HD 19525	1,20	-0,07	0,13	75	-0,11	0,14	3	1,11	1,30	-0,015
HD 19845	1,20	0,15	0,15	67	0,15	0,25	2	0,91	1,08	0,038
HD 20618	0,90	-0,18	0,13	73	-0,20	0,07	2	0,91	0,94	0,003
HD 20791	1,30	0,07	0,15	69	0,05	0,16	3	1,03	1,18	0,060
HD 20894	1,30	-0,05	0,14	77	-0,09	0,10	3	1,08	1,16	0,004
HD 21755	1,20	-0,09	0,13	71	-0,09	0,09	3	1,17	1,26	0,008
HD 22409	1,10	-0,21	0,12	77	-0,23	0,03	3	1,12	1,22	0,042
HD 22675	1,20	-0,06	0,13	72	-0,05	0,13	3	1,13	1,29	0,077
HD 22796	1,20	-0,07	0,14	73	-0,13	0,11	3	1,06	1,19	0,044
HD 23526	1,10	-0,10	0,13	70	-0,11	0,09	3	1,13	1,31	-0,001
HD 26409	1,30	0,06	0,14	66	-0,03	0,11	2	1,03	1,16	0,069
HD 27022	1,20	-0,02	0,14	78	-0,03	0,01	2	0,99	1,20	0,044
HD 27348	1,10	0,08	0,14	70	0,05	0,12	3	0,97	1,13	0,017
HD 27371	1,20	0,13	0,15	70	0,10	0,14	3	1,02	1,21	-0,001
HD 27697	1,30	0,11	0,15	71	0,07	0,15	3	1,03	1,16	0,010
HD 27971	1,20	0,06	0,15	68	0,01	0,15	3	1,03	1,23	0,020
HD 28100	1,40	-0,03	0,14	71	-0,03	0,13	3	1,15	1,23	-0,005
HD 28305	1,30	0,15	0,15	66	0,14	0,18	3	1,04	1,21	0,016
HD 28307	1,10	0,12	0,15	71	0,09	0,12	3	0,97	1,18	0,039
HD 29737	1,20	-0,41	0,13	71	-0,38	0,06	3	1,34	1,43	0,069
HD 30557	1,20	-0,01	0,15	69	-0,02	0,15	3	1,08	1,26	0,055
HD 30814	1,20	0,01	0,14	67	-0,05	0,14	3	1,09	1,28	0,029
HD 32008	0,90	-0,22	0,13	76	-0,17	0,15	3	0,91	0,98	0,025
HD 33833	1,20	-0,01	0,14	69	-0,07	0,10	3	1,04	1,20	0,051
HD 34538	0,90	-0,34	0,13	72	-0,34	0,05	3	1,06	1,25	0,029
HD 34559	1,20	0,03	0,15	70	0,01	0,13	3	1,00	1,15	0,028
HD 35369	1,20	-0,22	0,13	67	-0,27	0,07	2	1,23	1,23	0,045
HD 35410	0,90	-0,25	0,13	70	-0,21	0,10	3	1,15	1,32	-0,011
HD 36079	1,40	-0,22	0,15	70	-0,24	0,03	2	1,24	1,44	0,037
HD 37160	1,00	-0,58	0,13	73	-0,54	0,06	3	1,30	1,45	-0,007
HD 38527	1,10	-0,11	0,13	73	-0,10	0,10	3	1,04	1,15	0,041
HD 38656	1,20	-0,14	0,14	69	-0,17	0,12	3	1,16	1,31	0,069
HD 39004	1,30	0,05	0,14	74	0,04	0,16	3	1,04	1,16	0,028
HD 39007	1,10	0,07	0,15	71	0,01	0,16	3	1,00	1,15	0,039
HD 39019	1,20	0,20	0,15	67	0,14	0,15	3	0,86	1,06	0,045
HD 39364	1,10	-0,66	0,13	68	-0,63	0,07	2	1,46	1,49	0,050
HD 41361	1,60	-0,03	0,13	61	0,02	0,10	2	1,37	1,57	0,005
HD 41597	1,30	-0,53	0,13	65	-0,54	0,07	2	1,65	1,70	-0,003
HD 43023	1,10	-0,06	0,14	72	-0,02	0,13	3	1,04	1,16	-0,005
HD 43039	1,20	-0,26	0,13	72	-0,23	0,12	3	1,29	1,46	0,024
HD 45410	0,90	-0,09	0,14	80	-0,10	0,12	3	0,86	1,05	-0,012
HD 45415	1,20	-0,10	0,14	64	-0,10	0,16	3	1,19	1,38	0,042
HD 46241	1,20	-0,02	0,14	75	-0,04	0,11	3	1,09	1,25	0,001
HD 46480	0,90	-0,50	0,13	74	-0,50	0,04	2	1,05	1,11	0,036
HD 48432	1,00	-0,07	0,14	69	-0,14	0,10	3	0,98	1,18	0,055
HD 50522	0,80	0,06	0,15	70	0,07	0,22	3	0,98	1,19	0,021
HD 51000	1,20	-0,05	0,15	79	-0,04	0,06	3	0,96	1,03	0,053
HD 51814	1,40	0,02	0,14	70	0,00	0,15	3	1,24	1,37	0,011

Table 2. Continued.

Star	ξ	[FeI/H]	σ_{FeI}	n ₁	[FeII/H]	σ_{FeII}	n ₂	τ_{FeI}	τ_{FeII}	Σ
HD 53329	1,10	-0,42	0,13	71	-0,43	0,04	3	1,31	1,41	0,008
HD 54131	1,10	-0,12	0,14	69	-0,14	0,11	3	1,18	1,40	-0,013
HD 54810	1,00	-0,25	0,14	70	-0,27	0,06	3	1,20	1,40	-0,010
HD 55730	1,20	-0,13	0,14	70	-0,15	0,12	3	1,17	1,34	0,008
HD 57478	1,30	-0,02	0,14	73	0,11	0,03	2	1,19	1,43	0,041
HD 57727	1,00	-0,08	0,13	72	-0,10	0,09	3	0,97	1,13	-0,015
HD 58367	1,80	-0,10	0,13	58	-0,01	0,03	2	1,59	1,70	0,041
HD 60986	1,20	0,05	0,14	68	-0,02	0,11	3	0,98	1,11	0,065
HD 61363	1,20	-0,26	0,13	70	-0,27	0,13	3	1,27	1,42	0,053
HD 62345	1,20	-0,02	0,14	72	-0,05	0,09	3	1,09	1,22	-0,006
HD 62509	1,10	0,09	0,14	76	0,06	0,19	3	0,93	1,14	0,030
HD 64152	1,00	0,11	0,14	69	0,14	0,08	3	0,90	1,06	0,008
HD 65228	2,10	0,06	0,13	33	5,20	0,00	1	1,46	1,51	0,038
HD 65345	1,10	-0,01	0,14	73	-0,02	0,12	3	1,02	1,16	0,016
HD 65714	1,50	0,07	0,15	70	0,03	0,15	3	1,13	1,26	0,056
HD 67447	1,80	0,00	0,13	56	0,07	0,01	2	1,42	1,54	0,034
HD 68077	1,40	0,00	0,16	64	-0,01	0,18	2	1,13	1,27	0,075
HD 68290	1,10	0,07	0,14	77	0,04	0,13	3	0,91	1,07	0,049
HD 68312	1,20	-0,12	0,13	72	-0,11	0,13	3	1,10	1,18	0,062
HD 68375	1,10	-0,05	0,14	72	-0,06	0,08	3	1,00	1,14	-0,013
HD 71088	1,20	-0,05	0,15	68	-0,08	0,14	2	1,02	1,17	0,036
HD 71115	1,30	-0,04	0,14	74	-0,02	0,10	3	1,14	1,20	0,001
HD 71369	1,40	-0,08	0,14	73	-0,06	0,01	2	1,13	1,32	0,040
HD 73017	1,00	-0,47	0,13	72	-0,39	0,05	3	1,30	1,43	0,061
HD 73593	1,00	-0,18	0,13	69	-0,21	0,11	3	1,12	1,32	0,046
HD 74395	2,10	-0,04	0,13	45	-0,14	0,00	1	1,67	1,86	0,046
HD 74739	1,60	-0,04	0,15	51	-0,20	0,25	2	1,27	1,24	0,068
HD 74918	1,20	-0,12	0,13	73	-0,13	0,10	3	1,09	1,17	0,062
HD 75506	1,20	-0,31	0,14	69	-0,31	0,05	3	1,29	1,41	0,051
HD 76219	1,50	-0,09	0,15	60	-0,08	0,23	3	1,32	1,40	-0,016
HD 76294	1,20	-0,06	0,15	69	-0,06	0,14	3	1,20	1,37	-0,006
HD 76813	1,20	-0,04	0,14	69	-0,07	0,10	3	1,07	1,18	0,055
HD 77912	1,90	-0,10	0,14	51	0,02	0,12	2	1,60	1,69	0,051
HD 78235	1,10	-0,01	0,15	68	-0,08	0,05	2	0,94	0,89	-0,011
HD 78668	1,10	-0,03	0,14	69	-0,04	0,05	3	1,02	1,15	0,021
HD 79181	1,20	-0,26	0,14	73	-0,29	0,07	2	1,22	1,23	0,060
HD 79452	1,10	-0,69	0,11	77	-0,57	0,03	3	1,44	1,44	0,033
HD 80499	1,30	-0,06	0,13	71	-0,04	0,12	3	1,17	1,25	0,013
HD 81688	1,20	-0,29	0,13	70	-0,26	0,09	3	1,31	1,46	0,069
HD 82087	1,20	0,04	0,14	71	0,03	0,19	3	1,07	1,24	0,013
HD 82210	1,00	-0,21	0,13	77	-0,25	0,02	2	0,82	1,04	0,053
HD 82734	1,50	0,18	0,18	63	0,35	0,06	2	1,03	1,29	0,046
HD 82741	1,10	-0,16	0,14	69	-0,21	0,05	3	1,19	1,37	0,004
HD 83506	1,40	0,13	0,13	59	0,10	0,02	2	1,18	1,46	-0,010
HD 83805	1,20	0,04	0,15	68	-0,08	0,08	2	1,05	1,04	-0,013
HD 84441	1,70	-0,08	0,13	71	-0,11	0,00	1	1,36	1,28	0,047
HD 85444	1,20	0,01	0,17	72	0,01	0,05	3	1,08	1,18	0,007
HD 91190	1,20	-0,01	0,15	71	-0,04	0,14	3	1,08	1,22	0,015
HD 91612	1,10	-0,15	0,14	70	-0,18	0,05	3	1,14	1,28	0,021
HD 92125	1,90	0,02	0,13	64	-0,06	0,01	2	1,36	1,41	0,062
HD 93291	1,10	-0,07	0,13	70	-0,14	0,08	3	1,04	1,17	0,003
HD 94402	1,20	0,06	0,15	74	0,04	0,13	3	1,02	1,17	0,004
HD 94497	1,10	-0,12	0,13	75	-0,09	0,17	3	1,08	1,27	0,061
HD 95808	1,10	-0,06	0,13	74	-0,13	0,04	3	1,08	1,23	-0,005
HD 98839	1,60	-0,01	0,14	67	0,01	0,02	2	1,26	1,49	-0,008
HD 99055	1,20	-0,02	0,14	75	-0,05	0,09	3	1,07	1,17	-0,005
HD 99283	1,20	-0,14	0,13	75	-0,11	0,16	3	1,13	1,28	0,046
HD 99648	1,50	0,01	0,14	71	0,07	0,05	2	1,19	1,44	0,031
HD 100615	1,20	-0,10	0,13	73	-0,13	0,10	3	1,11	1,28	0,053
HD 100696	1,20	-0,31	0,13	73	-0,30	0,14	3	1,30	1,43	0,071
HD 100920	1,20	-0,16	0,14	67	-0,26	0,08	2	1,20	1,23	0,046

Table 2. Continued.

Star	ξ	[FeI/H]	σ_{FeI}	n ₁	[FeII/H]	σ_{FeII}	n ₂	τ_{FeI}	τ_{FeII}	Σ
HD 101484	1,10	0,04	0,14	68	0,01	0,12	3	1,01	1,20	0,039
HD 102070	1,40	0,06	0,16	71	0,07	0,22	3	1,08	1,19	0,052
HD 103462	1,10	-0,55	0,13	77	-0,45	0,07	3	1,38	1,44	-0,020
HD 103484	1,00	0,01	0,14	76	0,02	0,10	3	0,83	1,01	0,042
HD 104979	1,10	-0,39	0,14	69	-0,35	0,02	3	1,25	1,36	-0,009
HD 104985	1,20	-0,29	0,13	67	-0,32	0,03	2	1,24	1,32	0,042
HD 106057	1,20	-0,07	0,13	73	-0,08	0,12	3	1,09	1,22	0,053
HD 106714	1,20	-0,14	0,13	74	-0,17	0,08	3	1,16	1,27	0,024
HD 107383	1,20	-0,24	0,13	76	-0,23	0,11	3	1,20	1,34	0,030
HD 107950	1,50	0,04	0,14	70	0,05	0,02	2	1,12	1,31	0,020
HD 108225	1,20	0,04	0,15	69	-0,05	0,12	3	1,00	1,18	0,072
HD 109272	0,90	-0,22	0,14	74	-0,26	0,08	2	0,89	0,90	0,001
HD 109317	1,20	-0,01	0,15	74	-0,04	0,13	3	1,07	1,25	-0,009
HD 109379	1,50	0,01	0,14	70	-0,03	0,05	2	1,14	1,36	0,065
HD 110646	1,00	-0,40	0,13	77	-0,35	0,11	3	1,03	1,12	0,037
HD 111028	0,80	-0,01	0,14	75	-0,04	0,18	3	0,81	1,04	-0,006
HD 113095	1,20	-0,04	0,14	74	-0,04	0,16	3	1,06	1,20	0,026
HD 113226	1,30	0,09	0,15	71	0,04	0,12	3	1,03	1,15	0,009
HD 114256	1,30	0,02	0,15	72	-0,03	0,17	3	1,05	1,23	0,065
HD 115202	0,90	0,01	0,14	72	-0,04	0,19	2	0,87	0,99	0,064
HD 115659	1,30	-0,02	0,15	70	-0,03	0,16	3	1,14	1,23	0,029
HD 116292	1,10	-0,05	0,15	71	-0,06	0,10	3	1,11	1,29	-0,005
HD 116957	1,20	-0,09	0,13	75	-0,11	0,11	3	1,09	1,25	0,058
HD 117566	1,30	0,05	0,15	68	0,05	0,14	2	0,79	0,78	0,074
HD 117818	1,10	-0,27	0,13	72	-0,20	0,10	3	1,28	1,40	-0,002
HD 118219	1,10	-0,29	0,12	72	-0,25	0,11	3	1,29	1,40	0,015
HD 119126	1,20	-0,09	0,15	68	-0,21	0,09	2	1,21	1,27	-0,002
HD 119605	1,60	-0,31	0,14	70	-0,31	0,09	2	1,54	1,54	0,023
HD 120048	1,10	0,12	0,14	66	0,02	0,01	2	0,95	0,95	0,033
HD 120084	1,20	0,10	0,15	72	0,08	0,17	3	1,00	1,18	0,000
HD 120420	1,10	-0,16	0,14	75	-0,17	0,15	3	1,12	1,31	0,036
HD 120787	1,10	-0,32	0,13	75	-0,30	0,07	3	1,30	1,42	0,028
HD 125454	1,20	-0,06	0,14	74	-0,05	0,17	3	1,10	1,27	0,027
HD 126218	1,50	0,13	0,15	68	0,17	0,00	1	1,10	1,52	0,057
HD 127243	1,10	-0,71	0,12	76	-0,63	0,07	3	1,45	1,49	-0,007
HD 129312	1,40	0,07	0,15	67	0,10	0,04	2	1,09	1,38	0,001
HD 129336	1,20	-0,24	0,14	69	-0,27	0,04	3	1,18	1,31	0,080
HD 129944	1,10	-0,21	0,12	76	-0,18	0,10	3	1,19	1,31	-0,009
HD 129972	1,30	0,02	0,16	70	0,04	0,18	3	1,02	1,17	0,059
HD 130952	1,20	-0,35	0,15	74	-0,36	0,09	3	1,31	1,46	0,064
HD 131530	1,20	0,02	0,15	75	0,00	0,15	3	1,00	1,17	0,058
HD 132146	1,50	-0,05	0,13	70	0,01	0,00	2	1,27	1,48	0,037
HD 133002	0,90	-0,34	0,13	77	-0,30	0,04	2	0,86	0,67	0,033
HD 133208	1,50	-0,05	0,14	73	-0,05	0,03	2	1,24	1,48	0,048
HD 133392	1,20	0,10	0,15	73	0,07	0,19	3	0,99	1,18	0,009
HD 134190	1,20	-0,36	0,14	66	-0,39	0,09	2	1,36	1,31	0,004
HD 136512	1,20	-0,24	0,14	72	-0,28	0,07	3	1,26	1,43	0,023
HD 136956	1,40	0,10	0,15	72	0,16	0,06	2	1,06	1,32	0,000
HD 138716	0,90	0,01	0,14	74	-0,01	0,15	3	0,85	1,08	0,069
HD 138852	1,20	-0,19	0,13	74	-0,19	0,08	3	1,18	1,29	0,076
HD 138905	1,10	-0,27	0,13	75	-0,25	0,14	3	1,19	1,34	0,042
HD 139641	0,90	-0,48	0,12	77	-0,39	0,10	3	1,14	1,27	-0,003
HD 141680	1,20	-0,20	0,14	66	-0,29	0,06	2	1,26	1,31	0,038
HD 142091	0,90	0,10	0,14	75	0,10	0,22	3	0,78	1,03	0,044
HD 142198	1,20	-0,22	0,13	74	-0,16	0,13	3	1,25	1,41	0,032
HD 142531	1,20	0,09	0,15	72	0,01	0,15	2	0,96	1,13	0,009
HD 143553	1,00	-0,19	0,13	75	-0,21	0,16	3	1,05	1,24	0,051
HD 144608	1,50	-0,08	0,14	74	0,02	0,00	2	1,21	1,33	0,074
HD 145001	1,40	0,06	0,17	57	-0,10	0,17	2	0,93	0,93	-0,004
HD 146791	1,20	-0,05	0,14	74	-0,08	0,11	3	1,05	1,21	0,064
HD 147677	1,10	0,13	0,14	75	0,10	0,15	3	0,90	1,08	-0,005

Table 2. Continued.

Star	ξ	[FeI/H]	σ_{FeI}	n ₁	[FeII/H]	σ_{FeII}	n ₂	τ_{FeI}	τ_{FeII}	Σ
HD 147700	1,10	-0,07	0,14	75	-0,04	0,19	3	1,12	1,31	0,003
HD 148387	1,20	-0,02	0,14	76	-0,10	0,07	3	1,00	1,12	0,036
HD 148604	0,80	-0,15	0,13	79	-0,16	0,09	3	0,98	1,10	0,039
HD 148786	1,40	0,19	0,16	72	0,22	0,02	2	0,98	1,25	-0,010
HD 150030	1,60	-0,05	0,13	65	0,01	0,14	2	1,36	1,60	0,015
HD 150997	1,00	-0,09	0,13	75	-0,10	0,06	3	1,01	1,14	-0,034
HD 152815	1,20	-0,17	0,14	65	-0,25	0,05	2	1,21	1,23	0,057
HD 154084	1,20	-0,11	0,15	70	-0,17	0,12	2	1,11	1,26	0,003
HD 154779	1,40	0,10	0,16	74	0,06	0,18	3	1,00	1,11	0,023
HD 156874	1,20	0,01	0,15	76	0,03	0,18	3	0,97	1,12	0,049
HD 156891	1,20	0,13	0,15	72	0,15	0,22	2	0,88	1,04	0,064
HD 157527	1,20	0,08	0,14	72	0,13	0,17	2	0,92	1,00	0,057
HD 158974	1,30	-0,03	0,15	67	-0,08	0,16	2	1,20	1,18	0,019
HD 159181	2,10	-0,07	0,14	45	-0,12	0,00	1	1,75	1,95	0,038
HD 159353	1,10	0,04	0,13	73	-0,01	0,18	3	0,97	1,18	-0,015
HD 160781	1,40	0,05	0,16	50	-0,04	0,19	2	1,34	1,40	-0,011
HD 161178	1,20	-0,17	0,14	67	-0,25	0,07	2	1,25	1,29	0,035
HD 162076	1,10	0,06	0,14	74	0,02	0,10	3	0,90	1,06	0,005
HD 163532	1,30	-0,05	0,13	62	-0,06	0,22	3	1,28	1,47	0,015
HD 163917	1,40	0,11	0,15	71	0,10	0,20	3	1,04	1,19	0,037
HD 165760	1,30	0,01	0,14	62	-0,07	0,16	2	1,12	1,08	0,043
HD 167042	0,90	0,01	0,14	77	-0,06	0,10	3	0,76	1,00	0,025
HD 167768	1,10	-0,66	0,13	68	-0,52	0,07	3	1,44	1,51	0,031
HD 168656	1,20	-0,06	0,13	76	-0,04	0,12	3	1,10	1,18	0,051
HD 168723	1,00	-0,16	0,14	77	-0,15	0,14	3	0,90	1,08	0,024
HD 170474	1,20	0,03	0,14	75	-0,01	0,16	3	0,97	1,13	0,065
HD 171391	1,10	0,00	0,13	69	0,00	0,03	2	0,98	1,09	0,038
HD 174980	1,30	0,10	0,13	71	0,09	0,16	3	1,01	1,13	0,019
HD 176598	1,00	0,08	0,15	71	0,08	0,18	3	0,92	1,10	0,003
HD 176707	1,20	-0,24	0,14	65	-0,27	0,12	2	1,30	1,32	0,011
HD 177241	1,20	0,04	0,14	73	0,03	0,20	3	1,03	1,20	0,001
HD 177249	1,60	0,01	0,13	73	0,07	0,02	2	1,16	1,32	0,055
HD 180540	1,50	-0,01	0,15	60	-0,11	0,22	2	1,22	1,33	-0,019
HD 180711	1,20	-0,09	0,13	72	-0,09	0,13	3	1,10	1,26	0,040
HD 181276	1,20	0,05	0,14	75	0,07	0,20	3	0,96	1,12	0,060
HD 182694	1,20	-0,02	0,14	77	-0,03	0,09	3	1,08	1,17	-0,002
HD 182762	1,20	-0,05	0,13	77	-0,07	0,13	3	1,09	1,27	0,035
HD 183491	1,20	0,15	0,14	70	0,09	0,14	3	1,00	1,19	-0,001
HD 184010	1,00	-0,11	0,15	79	-0,10	0,14	3	0,85	1,04	0,016
HD 185018	2,10	-0,11	0,14	53	-0,08	0,00	1	1,63	1,74	0,049
HD 185194	1,40	0,05	0,13	69	0,12	0,13	2	1,14	1,42	0,016
HD 185351	1,00	0,02	0,14	78	0,03	0,16	3	0,83	1,01	0,005
HD 185467	1,40	0,12	0,16	69	0,13	0,25	2	1,00	1,15	0,055
HD 185758	1,70	0,00	0,12	71	-0,01	0,05	2	1,26	1,31	0,034
HD 185958	1,80	0,07	0,16	44	0,17	0,03	2	1,32	1,51	-0,001
HD 186675	1,30	-0,04	0,14	66	-0,12	0,11	2	1,15	1,12	0,043
HD 187739	0,90	-0,15	0,15	75	-0,15	0,23	3	1,07	1,29	0,017
HD 188310	1,20	-0,12	0,15	71	-0,17	0,10	2	1,08	1,25	0,007
HD 188650	1,80	-0,71	0,14	58	-0,60	0,05	2	1,70	1,70	0,071
HD 188947	1,20	0,09	0,15	74	0,05	0,19	3	0,99	1,20	-0,007
HD 189127	1,20	-0,15	0,14	65	-0,19	0,11	2	1,26	1,30	-0,016
HD 192787	1,10	-0,05	0,14	75	-0,06	0,11	3	0,98	1,12	0,045
HD 192879	1,20	-0,07	0,14	70	-0,04	0,13	3	1,09	1,24	0,040
HD 192944	1,40	-0,03	0,16	64	-0,11	0,11	2	1,15	1,11	0,056
HD 192947	1,20	0,04	0,14	74	0,04	0,19	2	0,94	1,06	0,059
HD 194013	1,20	-0,05	0,15	68	-0,17	0,08	2	1,09	1,12	0,046
HD 194577	1,20	0,02	0,15	68	-0,08	0,02	2	1,01	1,01	0,023
HD 196857	1,20	-0,22	0,14	75	-0,16	0,15	3	1,18	1,30	-0,005
HD 199665	1,00	-0,01	0,13	72	-0,01	0,10	3	0,95	1,11	-0,017
HD 200039	1,20	-0,10	0,15	76	-0,05	0,15	3	1,08	1,20	0,036
HD 201381	1,10	0,01	0,14	66	-0,12	0,05	2	1,00	1,04	0,020

Table 2. Continued.

Star	ξ	[FeI/H]	σ_{FeI}	n ₁	[FeII/H]	σ_{FeII}	n ₂	τ_{FeI}	τ_{FeII}	Σ
HD 203222	1,20	-0,02	0,14	75	0,06	0,17	3	1,01	1,10	0,068
HD 203387	1,20	0,06	0,14	77	0,09	0,11	3	0,87	0,94	0,048
HD 204381	1,20	-0,05	0,14	79	-0,05	0,12	3	1,00	1,10	0,013
HD 204771	1,20	0,08	0,15	77	0,03	0,17	3	0,91	1,10	0,064
HD 205072	1,20	-0,12	0,14	76	-0,11	0,10	3	1,09	1,19	0,020
HD 205435	1,10	-0,09	0,14	79	-0,05	0,11	3	0,94	1,05	0,050
HD 206356	1,20	0,11	0,14	75	0,06	0,12	3	0,94	1,13	0,026
HD 206453	1,30	-0,35	0,13	76	-0,34	0,10	2	1,29	1,31	0,051
HD 209396	1,20	0,05	0,15	77	0,00	0,12	3	0,96	1,13	0,052
HD 210354	1,20	-0,17	0,15	77	-0,18	0,11	3	1,22	1,40	0,018
HD 210434	1,20	0,15	0,16	70	0,11	0,26	2	0,89	1,07	0,026
HD 210702	1,00	0,01	0,15	78	0,00	0,21	3	0,81	1,03	0,053
HD 210807	1,30	-0,03	0,14	65	-0,08	0,14	2	1,10	1,19	-0,006
HD 211391	1,30	0,09	0,15	65	-0,05	0,06	2	1,05	1,09	0,055
HD 211434	1,20	-0,24	0,13	80	-0,25	0,09	3	1,12	1,20	0,045
HD 211554	1,50	0,09	0,14	63	0,02	0,00	1	1,14	1,26	0,028
HD 212271	1,10	0,10	0,15	77	0,11	0,12	3	0,89	1,07	0,017
HD 212320	1,30	-0,10	0,16	70	-0,02	0,20	3	1,12	1,19	0,051
HD 212430	1,20	-0,13	0,14	74	-0,16	0,09	3	1,15	1,27	0,022
HD 212496	1,00	-0,26	0,14	74	-0,23	0,14	3	1,22	1,42	-0,001
HD 213789	1,20	-0,02	0,14	73	-0,04	0,11	3	1,03	1,16	0,028
HD 213930	1,20	0,15	0,15	74	0,16	0,16	3	0,91	1,07	-0,001
HD 213986	1,10	0,11	0,16	74	0,11	0,23	2	0,90	1,11	0,000
HD 214567	1,10	-0,16	0,14	74	-0,19	0,02	3	1,10	1,21	-0,006
HD 214878	1,20	0,05	0,14	77	0,03	0,11	3	0,95	1,09	0,061
HD 215030	1,10	-0,43	0,14	66	-0,51	0,00	1	1,31	1,21	0,044
HD 215373	1,30	0,12	0,15	70	0,10	0,14	3	1,00	1,14	0,024
HD 215721	1,20	-0,44	0,12	76	-0,39	0,11	3	1,38	1,48	0,060
HD 215943	1,20	-0,02	0,14	75	-0,05	0,16	3	1,05	1,23	0,060
HD 216131	1,10	-0,02	0,13	72	-0,02	0,14	3	1,03	1,16	0,040
HD 217264	1,20	0,11	0,15	74	0,09	0,18	3	0,95	1,13	0,033
HD 217703	1,00	-0,15	0,14	77	-0,13	0,15	3	0,98	1,17	0,060
HD 218527	1,10	-0,29	0,14	79	-0,30	0,05	3	1,17	1,30	-0,021
HD 219139	1,20	-0,16	0,13	74	-0,16	0,11	3	1,17	1,32	0,026
HD 219615	1,20	-0,60	0,12	76	-0,47	0,11	3	1,41	1,50	0,043
HD 219945	1,20	-0,07	0,13	77	-0,09	0,11	3	1,09	1,26	0,002
HD 221345	1,30	-0,21	0,13	73	-0,21	0,16	3	1,17	1,32	0,070
HD 222093	1,30	-0,12	0,14	76	-0,16	0,16	3	1,14	1,31	0,073
HD 222387	1,10	-0,10	0,13	79	-0,10	0,12	3	1,01	1,14	0,021
HD 222574	1,90	0,06	0,13	55	-0,06	0,00	1	1,48	1,66	0,028
HD 223252	1,20	-0,01	0,14	77	-0,04	0,16	3	1,03	1,16	0,037
HD 224533	1,10	0,03	0,14	77	0,02	0,15	3	1,00	1,13	-0,003